Hindawi Publishing Corporation
EURASIP Journal on Wireless Communications and Networking
Volume 2006, Article ID 21297, Pages 1–23
DOI 10.1155/WCN/2006/21297

Cross-Layer Design and Analysis of Downlink Communications in Cellular CDMA Systems

Jin Yuan Sun, Lian Zhao, and Alagan Anpalagan

Department of Electrical and Computer Engineering, Ryerson University, Toronto, ON, Canada M5B 2K3

Received 1 October 2005; Revised 10 March 2006; Accepted 19 May 2006

A cellular CDMA network with voice and data communications is considered. Focusing on the downlink direction, we seek for the overall performance improvement which can be achieved by cross-layer analysis and design, taking physical layer, link layer, network layer, and transport layer into account. We are concerned with the role of each single layer as well as the interaction among layers, and propose algorithms/schemes accordingly to improve the system performance. These proposals include adaptive scheduling for link layer, priority-based handoff strategy for network admission control, and an algorithm for the avoidance of TCP spurious timeouts at the transport layer. Numerical results show the performance gain of each proposed scheme over independent performance of an individual layer in the wireless mobile network. We conclude that the system performance in terms of capacity, throughput, dropping probability, outage, power efficiency, delay, and fairness can be enhanced by jointly considering the interactions across layers.

1. INTRODUCTION

With the growing demand and popularity of high-speed data applications in wireless networks, the system capacity and bandwidth resource become increasingly stringent. Radio resource management plays a key role in wireless system design and analysis. Research efforts are made to expand the capacity and to efficiently allocate the resource. Some of the efforts include the evolution of the CDMA technology. For example, 3G (third generation) and 3G+ (beyond 3G) CDMA systems (i.e., WCDMA and CDMA2000) are superior to 2G CDMA systems (IS-95) in that the former ones have higher carrier bandwidth and faster power control frequency (more precise channel feedback). On the other hand, some efforts focus on the algorithm design which can be implemented in the software to optimize the system performance. As the research on 3G and 3G+ CDMA systems emerges, and although countless works have contributed to this research area, there still remain a great number of problems unsolved. In this paper, we would like to share our ideas to approach some of the problems in this field. We choose to focus on the cross-layer design of the CDMA networks as this issue has recently been capturing interests.

The traditional wireless networks mainly support voice service without data service provided through the Internet backbone. However, the integration of the wireless network and the wired backbone is of great importance today because of the increasing data application requirement at the mobile terminal (e.g., cellular phone and wireless laptop). While most previous research was on the performance optimization of individual layer, it often leads to performance degradation of other layers or suboptimal system performance. The hierarchical structure of the wireless networks, as the wired ones, facilitates us to design and study protocols for the single layer that is of particular interest since these layers (physical layer, link layer, network layer, transport layer, and application layer) are transparent to one another. But this isolation may cause suboptimal system performance. Recent research has shown that a well-designed cross-layer approach that supports multiple protocol layer adaptivity and optimization can yield significant performance gains [1]. Many researchers use the cross-layer approach for their designs. However, these designs can be very different due to various combinations and interactions of multiple layers.

We have studied a number of cross-layer approaches for CDMA system optimization in the literature. In what follows, we summarize some of these approaches. Authors of [2–8] propose cross-layer approaches to achieve system optimization in CDMA systems. In [2] a set of PHY-MAC (physical-MAC) mechanisms is proposed based on the rate adaptation provided by the MAC and the channel state from the PHY to improve spectrum efficiency and reduce power

consumption. Yu and Krishnamurthy [3] focus on cross-layer QoS (quality-of-service) guarantee by combining physical layer SIR (signal-to-interference ratio) and network layer blocking probability to reduce computational complexity and approximate the optimal solutions. Other works are also found to address physical/network cross-layer optimization issues [9, 10]. Price and Javidi [4] deal with the interaction between congestion (transport layer) and interference (MAC layer), and integrate them into a single protocol by means of rate assignment optimization. Friderikos et al. [5] interpret the rate adaptation as TCP-related since the rate in this paper is defined as the ratio of the current congestion window and RTT (round-trip-time) of the connection, and jointly considers it with physical layer (power). Hossain and Bhargava [6] model and analyze the link/PHY level influence on TCP behavior and illustrate their dependency. Yao et al. [7] study the reverse and forward link capacities balancing issue by covering link layer and the network layer to seek for optimal handoff probability. Chan et al. [8] propose a joint source coding power control and source channel coding, and interpret them as the MAC-layer power control and application-layer source coding, respectively, maximizing the delivered service quality and minimizing the resource consumption. There are also additional attention on other aspects of cross-layer design, such as to decrease the cross-layer interference [11] instead of optimization.

The above survey indicates that different interpretations of "cross-layer" and resources belonging to these layers produce a variety of cross-layer studies. While existing works address cross-layer issues based on two or three layers, we propose to fully address this issue by taking the four important layers into account: physical layer, link layer, network layer, and transport layer. We design algorithms/protocols for each of these layers by considering their communications and mutual impacts to prevent isolation thus improving the overall performance. At the physical layer, two fundamental techniques, power control and rate allocation, are studied. The proposed integrated power control and rate allocation is briefly introduced which is primarily used for the link-layer scheduling and is demonstrated in detail in the following scheduling schemes. At the link layer, a novel voice packet scheduling scheme named modified adaptive priority queuing (MAPQ) and a unified framework (UF) for scheduling hybrid voice and data traffic are proposed. An adaptive priority profile is defined in these schemes based on queuing delay and physical layer information such as required transmission power, and available transmission rate, which borrows the idea of composite metric from wired systems. Estimation error is considered when measuring received pilots at mobile stations. For MAPQ, this definition ensures system capacity improvement, packet dropping probability reduction, and fairness. Users are allocated resources according to their priorities in a modified PQ fashion constrained by total power budget of base stations. For UF, we address the consistency of the framework as well as the distinctions of voice and data scheduling processes by discussing the common policy and individual requirements of both classes. With this design, the proposed algorithm accomplishes system performance enhancement while retaining separate performance features without degradation. The uniformity of the proposed framework not only simplifies the implementation of the scheduling algorithms at base stations, but also is verified to be robust and resistant to various offered traffic load and variable service structure (voice/data proportion). At network layer, we propose an adaptive prioritizing soft handoff algorithm for concurrent handoff requests aiming at a same cell. A predicted set, an adaptive priority profile jointly exploiting the impact of required handoff power, and call holding time have been developed to realize the proposed algorithm. A link-layer scheduler residing in each base station to ensure the desired operation of the prioritizing procedure is also designed, with input information from network layer. At transport layer, we study the problem of TCP over wireless link and summarize the solutions for this problem from extensive research works. We design an algorithm to prevent the spurious timeouts at TCP sources caused by the stochastic intervals of wireless opportunistic scheduling.

The rest of this paper is organized as follows. Section 2 illustrates the system model based on which this research is carried out. The main body consists of Sections 3, 4, and 5, where we propose strategies for LINK/PHY (link/physical layer), NET/LINK/PHY (network/link/physical layer), and TRANS/NET/LINK (transport/network/link layer), respectively, and study their interactions. Section 6 gives out the simulation environment and the performance evaluation/analysis of the proposed cross-layer design. Finally Section 7 concludes this paper with primary contributions, open issues and certain limitations.

2. SYSTEM MODEL

We concentrate on a cellular WCDMA system with wrap-around cell structure, as shown in Figure 1, where mobile stations (MSs) select serving base stations (BSs, displayed as pentagrams) based on the measured strength of pilot signals (P_p) sent out periodically by BSs. Typically, 20% of the downlink total power will be assigned to pilot channel by each BS. The rest of the total power is shared by traffic channel and an other control channel (carries control information, power control symbols, etc.).

In forward link (downlink), BSs transmit packets to MSs through traffic channels which consist of frames. Each frame is of a 10 ms length and is subdivided by 15 time slots within one of which traffic destined for one specific MS is delivered.

To guarantee that MSs receive packets correctly, the transmission power allotted by BSs has to overcome channel impairments, which consist of path loss $(d_{ib}/d_0)^{-\alpha}$, shadowing $e^{-(\beta X_b)}$, and Rayleigh (fast) fading using Jakes' fading model [12], where d_{ib} is the distance between the MS and the BS, d_0 is the reference distance, α is the path loss exponent, $\beta = \ln 10/10$ is a constant, and X_b is a Gaussian distributed shadowing (in cell b) random variable with zero mean and variance σ_X^2.

Unlike the uplink case, downlink restriction is neither the intracell (from adjacent MSs within home cell) nor intercell (from neighboring other cells) interference, but the total

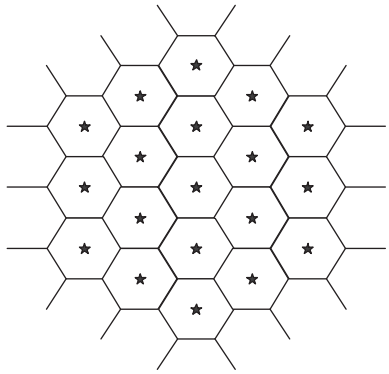

Figure 1: A typical cellular structure with base stations.

transmission power of BSs. Thus the E_b/I_0 (bit energy to interference density ratio), received at each mobile i from its home BS b, is expressed as

$$\gamma_i = \Gamma \frac{P_i G_{bi}}{(P_T - P_i) G_{bi} + \sum_{j \neq b} P_T G_{ji}}, \tag{1}$$

where $\Gamma = W/R$ is the spreading gain with W the spread spectrum bandwidth and R the required packet transmission rate. P_i and P_T (in *Watt*) denote the transmission power for user i and total downlink transmission power of BSs, respectively, assuming BSs are transmitting at the maximum capacity always. G_{i*} denotes signal attenuation (reciprocal to link gain) of the channel between user i and BS $*$. During each time slot, MS i compares the received γ_i with target E_b/I_0 γ^* and generates the power control command informing its serving BS to increase or decrease the transmission power. Note that unlike [13] and many others of its kind, we consider multipath fading as part of the channel impairments instead of using an orthogonality factor (OF) in (1). Authors of [13] argue that OF is defined as the fraction of received downlink power converted by multipath into multiaccess interference. They consider only the path loss as the channel impairment and include an OF to reflect the multipath impairment. Since the multipath impairment is reflected by fast fading, we do not employ OF here.

In reality, however, limited measuring ability of MSs can introduce an erroneous estimation of received pilots, which results in errors in measuring G_{i*} (obtained from measuring pilot signals). We approximate the sum of measurement errors as log-normally distributed as indicated in [14]. Let $e^{\beta Y_{ib}}$ denote the measurement error of the measured value, where Y_{ib} is a Gaussian distributed random variable with zero mean and a variance of σ_Y^2. As a result, the actual received SIR for each MS is derived from the following revised version of (1) counting errors:

$$\gamma_i = \Gamma \frac{P_i/P_T}{(1 - P_i/P_T) + e^{-\beta Y_{ib}} \sum_{j \neq b} G_{ji}/G_{bi}}. \tag{2}$$

3. LINK-LAYER PACKET SCHEDULING (LINK/PHY)

Packet scheduling is a promising link-layer management mechanism. More and more research [15, 16] on this technique has emerged. However, existing algorithms focus on data scheduling with little or no concern on voice. The time-varying nature of wireless channels determines the importance of voice scheduling. Voice dropping is less likely to come from congestion than data dropping due to its higher priority. Nevertheless, voice traffic is prone to suffer a deep-fading channel and consumes a large amount of limited base station power, thus must be scheduled properly. In the first part of this section, we propose a novel voice scheduling scheme named modified adaptive priority queuing (MAPQ) for forward link in a wireless cellular WCDMA environment. An adaptive priority profile is defined in the scheme based on queuing delay and required transmission power, which borrows the idea of composite metric imported by IGRP (interior routing protocol) and EIGRP (enhanced IGRP) from wired networks.

Next, we present a unified packet scheduling framework (UF) to include data traffic and demonstrate the easy integration and general adaptability of MAPQ to the UF.

The E_b/I_0 used here is the same as (1) except that R in $\Gamma = W/R$ here, $R \in \{R_v, R_d\}$, is the required transmission rate of voice or data packets. The actual received E_b/I_0 for each MS takes the form of (2).

For link-level scheduling implementation, each BS has a scheduler to regulate incoming hybrid traffic, and arrange packets aimed for MSs in a specified sequence depending on the logic of the scheduler. The scheduler implemented in BSs is sketched in Figure 2, where Q_{V1} and Q_{V2} denote voice queues while Q_{D1} and Q_{D3} denote data queues.

3.1. Integrated power control and rate allocation

We propose to use physical-layer information power/rate as the input for link-layer scheduling (LINK/PHY).

Fast closed-loop power control (CLPC) is applied to our scheme in the downlink to optimize the system performance. The merit of CLPC has two aspects compared to the alternative open-loop power control (OLPC).

(1) Under relatively good channel conditions, where fast fading is not severe, the transmission power for mobiles from the base station can be kept to the minimum required level to satisfy the SIR at all times since CLPC performs faster than channel fading rate. Thus, CLPC is able to compensate medium to fast fading and inaccuracies in OLPC [17]. As a result, more transmission power of the base station remains for voice users that are either far away from the base station or in a difficult environment, and data users, giving rise to enhanced system capacity and data throughput in multimedia networks.

(2) Under poor channel conditions where users undergo severe fast fading, OLPC may fail to adapt to the required transmission power for each mobile due to the slow rate and inaccuracy of OLPC, resulting in an insufficient power level to combat channel fading and fulfill QoS requirement.

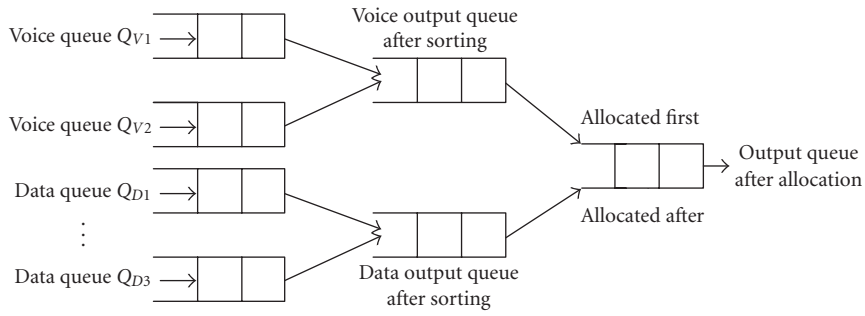

Figure 2: Base station scheduler structure for scheduling framework.

Whereas our approach CLPC solves this problem because the transmission power is always adjusted accordingly to satisfy the QoS requirement.

Single-code variable spreading gain (VSG) rate allocation technique is applied to our scheme, as demonstrated later, to adjust the transmission rate when the satisfaction cannot be achieved by power adaptation only. According to the calculation of the transmission rate R after spreading, $R = W/\Gamma$, where W and Γ represent the spread spectrum bandwidth and the spreading gain, respectively, the actual transmission rate that is obtained can be adjusted by different values of Γ, given the fact that W is a constant. Typically, in the WCDMA standard, $\Gamma \in \{4, 8, 16, 32, 64, 128, 256, 512\}$. The actual value assigned to Γ depends on the transmission rate demanded. Note that R is inversely proportional to Γ. When we select a smaller Γ, we will obtain a larger R, and vice versa.

The way that we combine power and rate for our scheduling scheme is to first adjust power with a fixed rate to the point that the change of power no longer produces any effect on the scheme (see Section 3.2.2). Then the power is fixed and the spreading gain will be adjusted to obtain the satisfactory transmission rate and to fulfill the predefined goal. More details will be given in the description of the voice/data framework.

3.2. MAPQ and UF

3.2.1. Voice only: MAPQ

In general, MAPQ has two subprocesses: sorting and allocation. The operation of MAPQ scheme and its subprocesses is demonstrated as follows.

MAPQ scheduler sorts incoming traffic into high- (Q_{V1}) and low- (Q_{V2}) priority queues based on each packet's calculated priority value, which is evaluated by jointly considering required power and buffering delay as $\text{AP}_i = a * \text{delay}_i^{\text{nor}} + b/\text{power}_i^{\text{nor}}$, where AP_i denotes the adaptive priority for packet i. $\text{delay}_i^{\text{nor}}$ and $\text{power}_i^{\text{nor}}$ are the normalized buffering delay and the normalized required power of packet i, respectively. The buffering delay is defined as the time interval of the arrival and departure of a packet. For simplicity, the calculation time of the scheduler is neglected for all packets in the simulation. Zero buffering delay means that the packet gets served in the first round upon arrival. Let $\text{delay}_i\ V_{\text{thre}}$ denote the buffering delay of packet i, the delay threshold of voice beyond which voice packets enter Q_{V1}. This step is implemented in the scheduler programming. It does not indicate the actual packet movement in the memory where the queues locate. Let power_i and $\text{power}_{\text{mean}}$ denote the required transmission power of packet i, and the mean downlink transmission power of active users in one cell. Then we have $\text{delay}_i^{\text{nor}} = \text{delay}_i/V_{\text{thre}}$, and $\text{power}_i^{\text{nor}} = \text{power}_i/\text{power}_{\text{mean}}$. The way to normalize the delay and power components in the AP expression ensures the two terms in AP ($a * \text{delay}_i^{\text{nor}}, b/\text{power}_i^{\text{nor}}$) comparable. Parameters a and b are the adaptive factors determining the weight of delay over power (wdp, in our case voice is delay sensitive thus a larger wdp should be assigned). The smaller required power (the better channel condition), or the larger delay, yields the higher priority (AP). The way to define the priority profile ensures users with better channels and larger delays to get served first, thus increases the throughput, reduces the voice packet dropping probability, and guarantees the fairness which is measured by the mean delay in the network.

MAPQ scheduler then allocates resources starting from Q_{V1} according to AP values and total transmission power budget of BSs. The scheduler does not terminate even if the user currently being served in Q_{V1} requires a power exceeding the remaining budget. Since each user's priority depends on both delay and power, higher priorities do not merely indicate smaller powers. Also, after Q_{V1} has been fully checked and if there is power remaining (P_r), the scheduler will continue to check Q_{V2} and serve available users in Q_{V2} using P_r. This is the major difference between MAPQ and classic PQ. A similar concept can be found in [18], where the authors proposed a modified FIFO scheme for power-constraint systems. This modified queuing fashion can lead to higher-power utilization efficiency, as will be shown later.

3.2.2. Unified voice/data framework: UF

The rest of this section is dedicated to the discussion of the UF. In the proposed framework, the allocation scheme is applied to not only each queue within each class but also

among classes. It is apparent that voice class has higher priority than data class, which necessitates the employment of the proposed allocation algorithm (modified PQ) for each voice queue to secure the scheduler not skipping to data class before completing checkup within voice class. However, classic priority queuing scheduler will not jump to data users until all the voice users have been served. It may cause power waste if none of the users in voice queues but some of the users in the data queue can be served. The proposed allocation algorithm further improves system capacity and throughput by also performing an exhaustive search within data class after an exhaustive search within voice class. We do not repeat the similar part of scheduling in terms of sorting and allocation for data traffic but would like to emphasize the discrepancy of data scheduling (sorting and allocation) as follows.

Difference in sorting mainly lies in the expression of adaptive priority profile. We have for data

$$\mathrm{AP}_i = a * \mathrm{delay}_i^{\mathrm{nor}} + b/\mathrm{power}_i^{\mathrm{nor}} + c/\mathrm{rate}_i^{\mathrm{nor}}, \quad (3)$$

where AP_i denotes the adaptive priority for packet i, and a, b, and c are adaptive constants. Voice and data have different a, b, and c values. Note that "$\mathrm{rate}_i^{\mathrm{nor}}$" denotes the normalized new required transmission power after decreasing the data rate, using (1), where $\Gamma = W/R_d$. The normalization method is similar to that used for voice power normalization. Here we use "$\mathrm{rate}_i^{\mathrm{nor}}$" in order to distinguish from $\mathrm{power}_i^{\mathrm{nor}}$ in the AP expression. Furthermore, "$\mathrm{rate}_i^{\mathrm{nor}}$" is used to emphasize that the new required transmission power is obtained by adjusting the data rate.

Voice requires constant bit rate during transmission and thus it is unlikely to change voice users' priority through rate variation. On the other hand, data (best-effort traffic in this paper unless otherwise specified) transmission rate is variable and can be raised if extra power is available or reduced without enough power resource to support target rate. In data scheduling profile, the last term "c/rate_i" is not used until delay exceeds a predefined threshold D_{thre}, and the required transmission power is still too large to increase AP. If the packet enters this stage (delay $> D_{\mathrm{thre}}$), it implies that merely adjusting power does not get an opportunity for the packet to be transmitted. At this point, transmission rate is adjusted since the change of power only no longer produces any effect. This is the only case where we decrease the required transmission data rate in order to get a smaller required power while SIR target is maintained. Since data users are able to withstand some delay and do not have strict drop bound, in which case wdp should be less than 1 to serve users under desirable channel conditions (small transmission power) with preference.

For simplicity, we set a to 1 and adjust b in the range of $(0, 1)$ for voice. For data, a is set in the range of $(0, 1)$ while b (or c) is set to 1. We compare to show the sorting subprocesses and allocation/reallocation subprocesses of voice and data scheduling in Figures 3 and 4. We observe in Figure 3 that the sorting processes for voice (Figure 3(a)) and data (Figure 3(b)) scheduling are similar. While Figure 4 illustrates more complex data allocation process (Figure 4(b)) because of the additional reallocation process.

In the particular reallocation, process data scheduler does not stop when the remaining power is not enough to support the current packet, because data transmission rate is adjustable according to the amount of remaining power resource as indicated earlier. Hence, the remaining power (if any) can be further allocated to specially selected data users with various transmission rate values. The idea behind is summarized as follows. After every packet in the queue has been checked, if there is remaining power for one more "normal" packet even at minimum rate, this packet gets served (system capacity increased). If not, share the power left among "normal" packets since they require lesser power (data throughput improved). Only if neither of the above is true, we give the extra power to the first "moderate" or "urgent" packet in the sorted output queue. This packet has already been allocated resource after all packets in the data queue have been scheduled. P_r is not allotted to "moderate" or "urgent" packets which are still in the queue since they consume relatively large powers. As queuing delay increases, they will be assigned a larger AP until eventually get transmitted. This is the key role of delay taken into account in our design.

4. NETWORK LAYER ADMISSION CONTROL AND SOFT HANDOFF (NET/LINK/PHY)

High mobility and universal access are enabled by handoff mechanisms employed in next-generation cellular CDMA networks. Without handoff, forced termination would occur frequently as mobile users traverse cell boundaries.

An apparent pair of contradictive parameters representing resource management efficiency and effectiveness in a handoff system is the call blocking probability (P_b) and the handoff dropping probability (P_d). Since fixed downlink total traffic power is shared between newly accepted users and ongoing handoff users, one's being greedy will induce another's being starved. It is therefore important to regulate and optimize their behaviors by balancing the amount of resources distributed. Based on the fact that interrupting an ongoing call is more disagreeable than rejecting a new call, handoff users are issued higher priority to reduce P_d wherever competition arises. Among numerous prioritizing algorithms [19, 20], resource reservation has attracted an overwhelming favor owing to lighter required communication overhead. However, existing algorithms prioritize handoff users as an entire category towards new users category. None of them concerns priority assignment among handoff users, which is necessary when several users attempt to handoff to a same target cell simultaneously, under the constraint of limited available target cell power (guard power P_G) set aside for handoffs. By "simultaneously" we mean while the BS is still handling one handoff request, another one or several requests may emerge, and so forth over and over. This is especially true in metropolitan cities where the mobile networks are mostly busy with cellular phone users. It does not mean two or more requests emerging at exactly the same time instant, which is not very likely in reality. Therefore, it is imperative to avoid signaling flood at the moment of

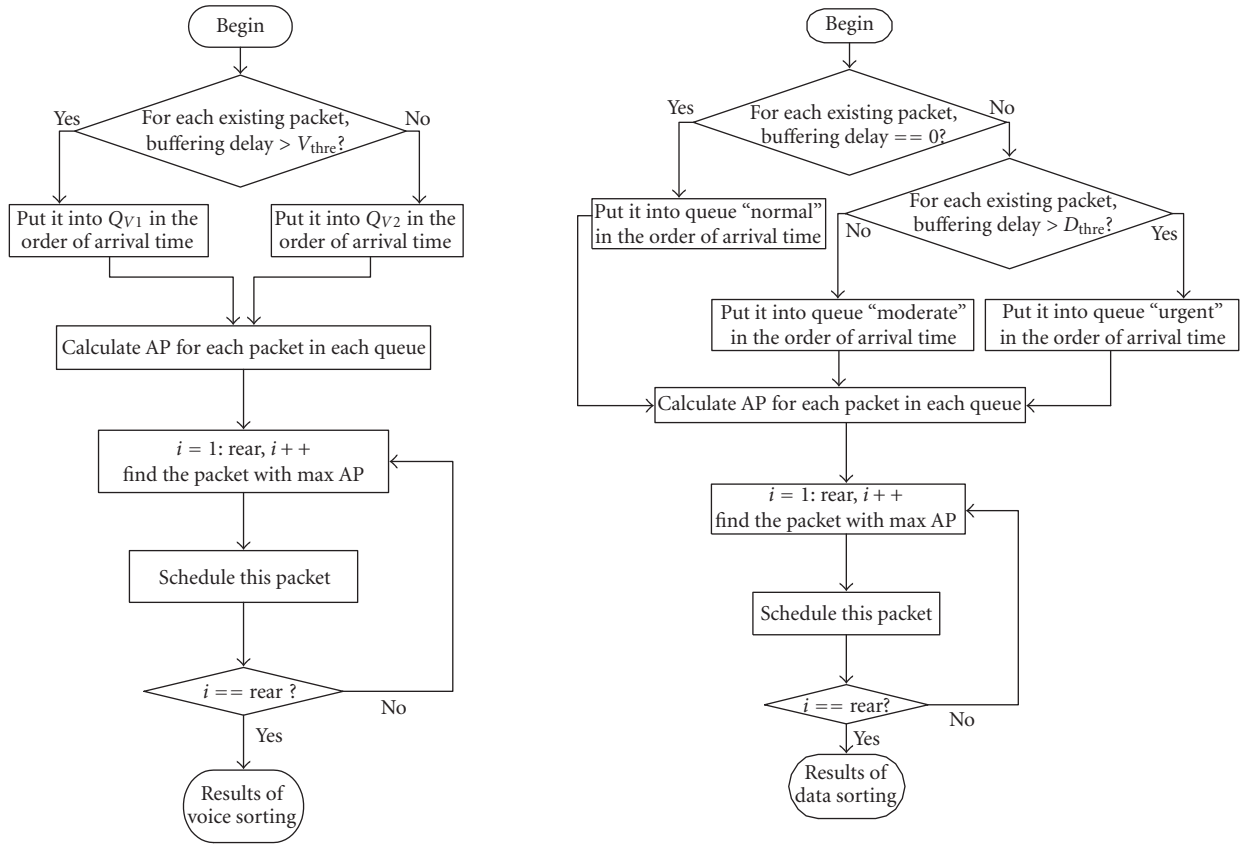

(a) Sorting subprocess of voice scheduling

(b) Sorting subprocess of data scheduling

Figure 3: Sorting processes.

simultaneous handoff requests, since predictions would not occur at the same time. Please refer to [21] for detailed explanations about the motivation and necessity of the proposed prioritizing algorithm.

We propose a handoff prioritizing algorithm, employing a link-layer scheduler with network and physical layer input (NETWORK/LINK/PHY). For prioritizing handoff users, a scheduler implementing link-layer scheduling with network-layer inputs inheres in each base station to regulate incoming handoff requests and to arrange these messages designated to different target BSs in a specified sequence depending on the logic of the scheduler, which has been proposed with physical-layer inputs in the previous section. The scheduler applied to BSs is sketched in Figure 5, assuming the current serving base station is BS_0. $BS_1, BS_2, \ldots, BS_n$ denote target handoff BSs, with n the number of handoff base station targets.

4.1. Connection admission control (CAC)

Capacity of CDMA systems is "soft." Acceptance of each new call increases the interference level of existing ongoing calls and affects their quality [22]. Hence, CAC is deployed to control the access to such networks, complying with types of service and quality-of-service (QoS) requirement, as well as current system load.

With wireless Internet applications growing, the forward link becomes very critical to system capacity, in that the bottleneck-like power capacity of BSs imposes stringency on available power resources allotted to each sharing user. The CAC mechanism employed in this paper, thereby, is based on total downlink traffic power and the precedence of handoffs over new calls, which is shown as a handoff request is admitted if

$$\sum_{i=1}^{N_{\text{on}}^c} P_i + P_{\text{ho}} \leq P_t, \tag{4}$$

and a new connection request is admitted if

$$\sum_{i=1}^{N_{\text{on}}^c} P_i + P_{\text{rsv}} + P_{\text{new}} \leq P_t, \tag{5}$$

where N_{on}^c is the number of ongoing calls in cell c, and P_i, P_{ho}, P_{rsv}, P_{new}, and P_t represent the required power of an ongoing call i, the incoming handoff call, the reservation for future handoffs (will be discussed later), the incoming new call, and the downlink total traffic power of BSs, respectively. Both (4) and (5) conform to the general admission criterion $\sum_{i=1}^{N_{\text{on}}^c} P_i \leq P_t$.

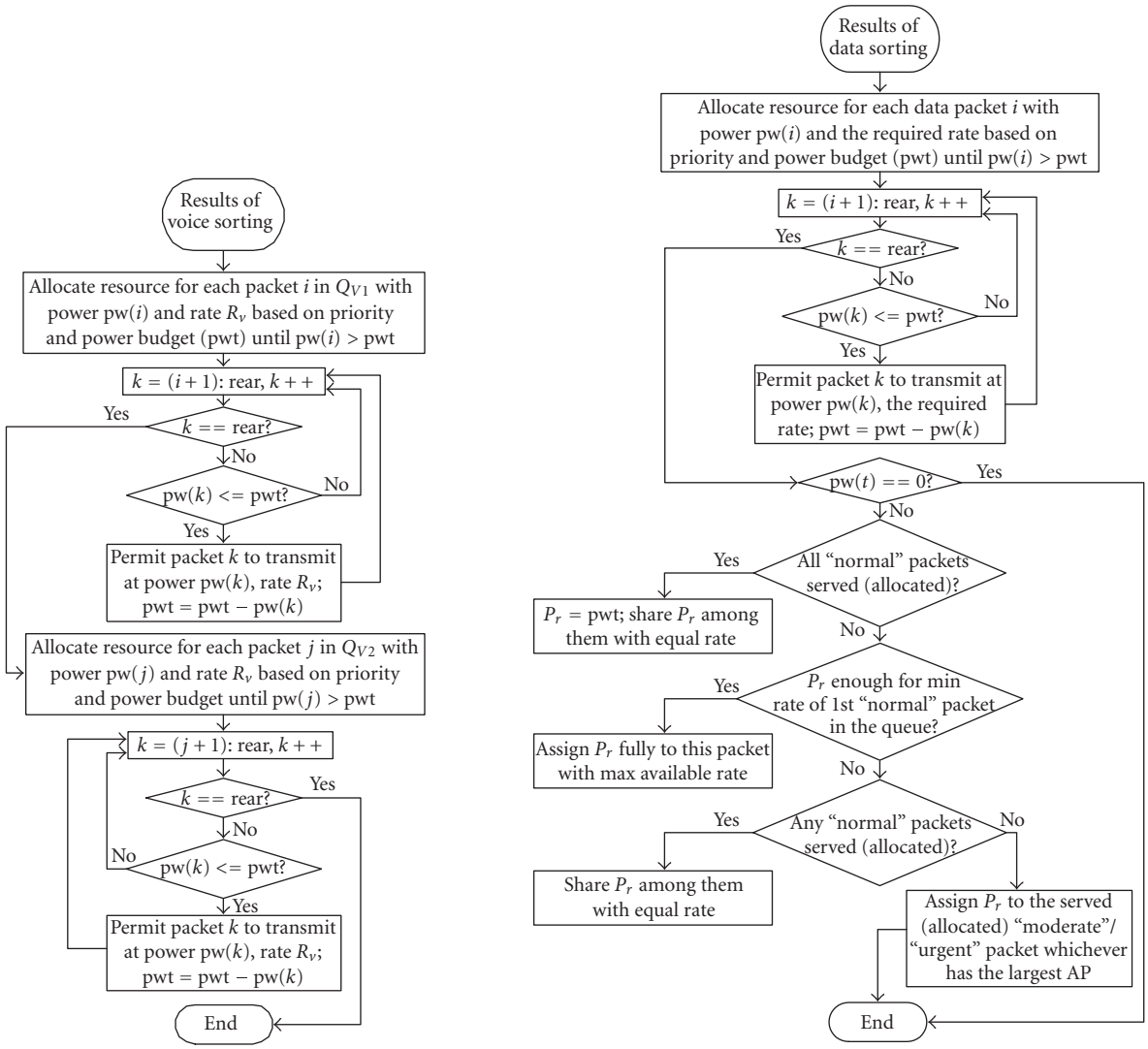

(a) Allocation subprocess of voice scheduling

(b) Allocation and reallocation processes of data scheduling

Figure 4: Allocation processes.

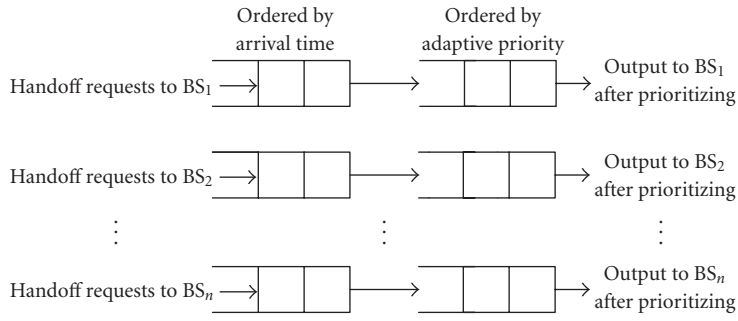

Figure 5: Base station scheduler structure for handoff algorithm.

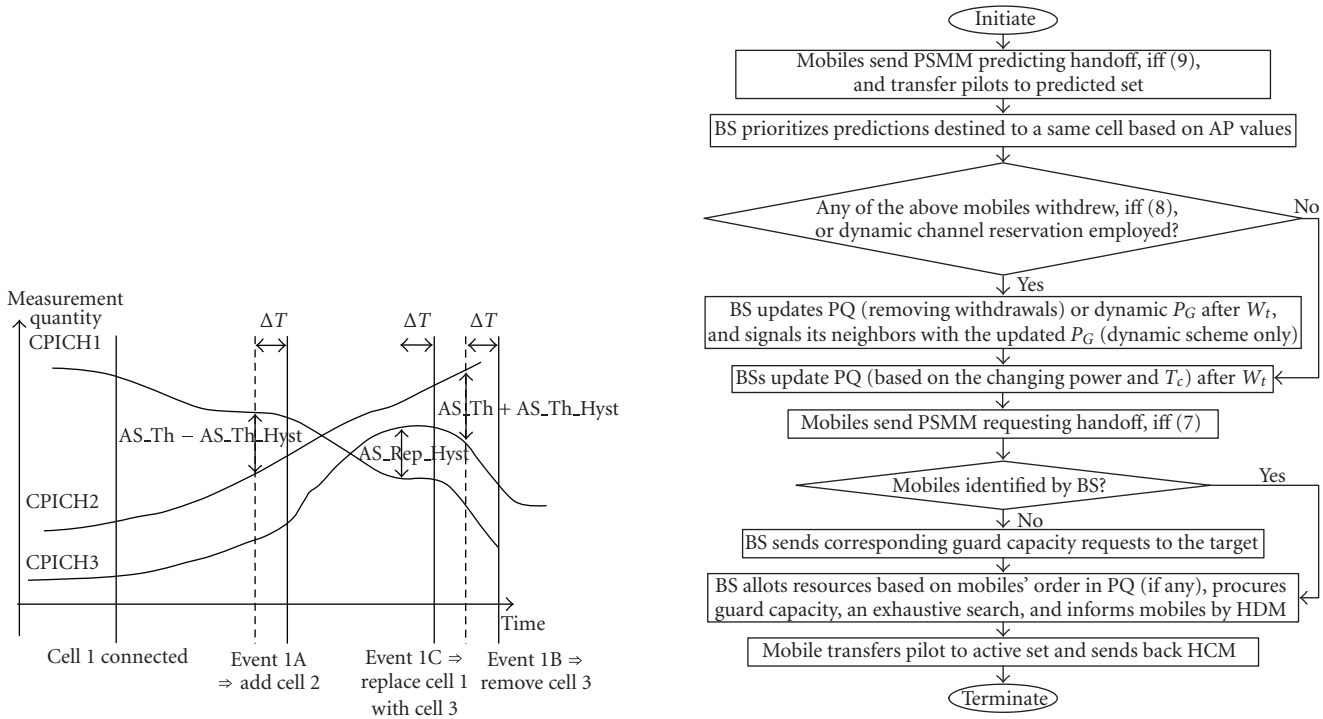

(a) A typical soft handoff algorithm

(b) Proposed soft handoff procedure

Figure 6: Soft handoff algorithm and procedure.

4.2. Soft handoff

One of the major benefits of a CDMA system is the ability of a mobile to communicate with more than one base station at a time during the call [23]. This functionality allows the CDMA network to perform soft handoff. In soft handoff a controlling primary base station coordinates with other base stations as they are added or deleted for the call. This allows the base stations to receive/transmit voice packets with a single mobile for a single call.

In forward link handoff procedure, a mobile receives pilots from all the BSs in the active set through associated traffic channels. All these channels carry the same traffic (with the exception of power control subchannel [23]), which facilitates the mobile to gain macroscopic diversity by combining power received from the channels (i.e., maximal ratio combining [24]). Thus, less power is needed implying total interference lessening and system capacity raising.

A basic soft handoff algorithm typically used in 3G CDMA systems is illustrated in Figure 6(a) [25], with AS_Th, AS_Th_Hyst, AS_Rep_Hyst, and ΔT defined as the threshold of reporting for active set transfer, hysteresis of the former threshold, replacement hysteresis, and time to trigger, respectively. CPICH is the abbreviation of common pilot channel. The events, together with the hysteresis mechanism and time to trigger mechanism are discussed in [25].

We employ a similar basic algorithm with slight simplification. The selection of a base station into the active set and the deletion from the active set are based on dynamic thresholds. Let M_{ps}^{b} and $\text{Best}_{\text{ps}}^{\text{active}}$ be the measured pilot signal from base station b, and best measured pilot from the active set, respectively. All the variables appearing in the inequalities below have the unit of *Watt*. A base station b is added into the active set if

$$M_{\text{ps}}^{b} > \text{Best}_{\text{ps}}^{\text{active}} - \text{AS\_Th} + \text{AS\_Th\_Hyst}, \tag{6}$$

for a period of ΔT, and is removed from the active set if

$$M_{\text{ps}}^{b} < \text{Best}_{\text{ps}}^{\text{active}} - \text{AS\_Th} - \text{AS\_Th\_Hyst}, \tag{7}$$

for ΔT, where AS_Th, AS_Th_Hyst, and ΔT are design parameters.

We briefly describe the mobile-assisted soft-handoff procedure as follows: mobile detects pilot strength from its monitored set by (6) and sends a pilot strength measurement message (PSMM) to the serving BS. BS requests resources from the target handoff cell, allocates traffic channel, and sends a handoff direction message (HDM) to mobile. Mobile transfers this pilot to the active set and transmits to BS a handoff completion message (HCM). Mobile starts handoff drop timer when the pilot strength in the active set meets (7) and sends to BS a PSMM. Mobile removes the pilot from the active set to the monitored set as the above time expires.

Note that the monitoring mechanism enables us to perform the prediction for prioritizing without extra network resources or high cost, as will be discussed in the next section.

4.3. Adaptive prioritizing soft handoff algorithm

The parameters and performance measures of the proposed prioritizing algorithm are addressed in this section, together with the description of the detailed implementation procedure of the algorithm. We mentioned in Section 1 that the adaptive priority profile is designed by jointly considering several elements, which are critical to define a specific handoff user.

4.3.1. Prediction

First of all, user mobility and location information are needed by prediction, which is the prerequisite of the prioritizing algorithm. This information is utilized by predictions for reserving guard capacity in the literature to track the speed and moving direction of mobiles. However, Wang et al. [19] claimed that such information procured from mobility models or GPS monitoring is generally costly and inaccurate, and complicated as well. As an alternative, they proposed using measured pilot strength to predict handoff (in IS-95 systems) since it is the origin of every handoff thus is accurate. Moreover, it is inexpensive since no additional network signaling is needed. We take advantage of this idea for the prediction in our algorithm, but modified it for 3G CDMA systems (i.e., WCDMA). It must be noted that the prediction method introduced in this paper is not as complex and precise as the aforementioned one because our focus is not on guard capacity reservation algorithm. However, with elaborately designed prediction scheme the significance and effectiveness of our algorithm will be more prominent.

Typically, in addition to the avoidance of signaling flood, prediction is updated at the end of every prediction window W_t to remove withdrawals (i.e., (7) holds) resulting from incorrect predictions or call termination ($T_c > D_{\text{th}}$, see Section 4.3.3 below). The output priority queue (PQ) is updated accordingly based on the latest information procured through prediction notification from mobiles. When handoffs actually take place, mobiles which are in PQ are identified by BS and are allocated channels immediately if the guard power allows. On the other hand, if the handoff requests are not identified as in the regular handoff procedure, these requests have to be sent to the target cell first since the BS has to inform the target to reserve power resources, where there exists the uncertainty about whether these requests can be approved with sufficient resources. Hence with prediction, the availability of resource is assured to maintain dropping performance. The handoff execution delay is also shortened which may cause power outage and fade margin enlarging [26]. Note that it is wise to shorten this delay by all means especially in our case. Since additional handoff execution time can be caused by queuing and sorting the handoff predictions in the proposed algorithm, which may introduce computation complexity to the base station and reduce the base station's handoff processing speed, all of the above reasons reinforce the need for prediction.

A predicted set is proposed in our algorithm, which consists of BSs satisfying the inequality beneath,

$$M_{\text{ps}}^{b} > \lambda\left(\text{Best}_{\text{ps}}^{\text{active}} - \text{AS\_Th} + \text{AS\_Th\_Hyst}\right). \tag{8}$$

The prediction threshold PS_Th obeys the dynamics of the threshold for the active set switching, and is related by $\text{PS\_Th} = \lambda(\text{Best}_{\text{ps}}^{\text{active}} - \text{AS\_Th} + \text{AS\_Th\_Hyst})$, where λ, $\lambda \in (0, 1)$ is a design constant affecting the prediction threshold above which the pilot is added into the predicted set, relative to the active set threshold. The criterion (8) serves as a trigger for the execution of the prioritizing algorithm. When (8) is satisfied, MS will report to BS of the prediction and the call holding time T_c, and the request will be put into the priority queue. As long as the queue is not empty, BS will perform the algorithm at the end of W_t.

4.3.2. Downlink transmission power

Next, channel condition should be taken into account of the profile, in that it is the indicator of required handoff power. A user experiencing better link gain and hence demanding less power is given a higher priority, in order to get more users served with the same amount of scarce downlink power resource. Assuming the maximum size of the active set is 2 (i.e., at most 2 BSs co-serve a handoff user at the same time), we can apply the maximal ratio combining strategy in (1) to derive the E_b/I_0 of a mobile i within the soft handoff zone as

$$\gamma_i = \sum_{b=0,1} \Gamma \frac{P_{bi} G_{bi}}{(P_T - P_{bi}) G_{bi} + \sum_{j \neq b} P_T G_{ji}}, \tag{9}$$

where 0 and 1 are in general the two coserving base station's identity numbers and P_{bi} is the transmission power to mobile i from BS b (current BS 0 and target BS 1). The actual received E_b/I_0 takes the form of (2). Based on the straightforward power division strategy [27] (i.e., $P_{0i} \doteq P_{1i}$), under the presumption of $\sum_{j\neq 0} G_{ji}/G_{0i} \doteq \sum_{j\neq 1} G_{ji}/G_{1i}$, the required handoff power from BS1 to mobile i can be written as

$$P_{1i} \doteq \frac{\gamma_i P_T \left(1 + \sum_{j\neq 1} G_{ji}/G_{1i}\right)}{2\Gamma + \gamma_i}. \tag{10}$$

4.3.3. Call-holding time

The last term included in the profile is the call-holding time T_c. This information can be easily derived by the UE (user equipment) through monitoring the connection time elapsed for the ongoing call. For the proposed profile, we import a parameter D_{th} denoting the death threshold for ongoing calls. The ongoing call is presumed to be terminated by the user before the actual handoff takes place if its T_c is greater than D_{th} at the time the prediction is made. If $T_c < D_{\text{th}}$ holds at the time of prediction, higher priority is assigned to a longer T_c. Because it is more probable that this mobile will terminate its call soon and release the resource for other mobiles' use.

We finally conclude the adaptive priority profile for user i as

$$\mathrm{AP}_i = \frac{1}{\mu P_{1i}^{\mathrm{nor}}} + T_{ci}^{\mathrm{nor}}, \tag{11}$$

in which AP_i is the user i's priority and μ is the adaptive factor adjusting the proportion of power and time to be comparable quantitatively. P_{1i}^{nor} and T_{ci}^{nor} denote the normalized downlink transmission power and the normalized call holding time of user i, respectively. $P_{1i}^{\mathrm{nor}} = P_{1i}/P_{\mathrm{mean}}$, where P_{mean} is the mean downlink transmission power of predicted handoff users for the same target cell. $T_{ci}^{\mathrm{nor}} = \lceil T_{ci}/T_{\mathrm{scale}} \rceil$, where $T_{\mathrm{scale}} = 10\,\mathrm{s}$ is the scale of the calling time. We use a rough calling time measuring method. The available T_{ci}^{nor} values are $0, 1, 2, \ldots, D_{\mathrm{th}}/T_{\mathrm{scale}}$. While the actual T_{ci} values can be any number between 0 and D_{th}, for simplicity, we assume that the $T_{ci}/T_{\mathrm{scale}}$ values will be ceiled to one of the above T_{ci}^{nor} values for the AP calculation. This definition style is derived from the wired networks, where IGRP and EIGRP routing protocols define a composite metric associated with each route in an alike fashion as mentioned in Section 3. Specifically, we subdivide users into two classes, which are distinguished by different priority profiles. According to Viterbi et al. [28], the maximum fade margin (max γ_d) put apart for overcoming shadowing correlation (with coefficient a^2) is obtained at the cell boundary, subject to a certain outage probability target (P_{out}^*). Hence, we issue boundary users a lower μ since they require a higher power for handoff (due to a higher γ_d) to ensure fairness. For convenience, we set $\mu = 1$ for ordinary users and $\mu \in (0, 1)$ for marginal users. Dedicated surveys on fade margin improvement and delicate relations among parameters such as γ_d, P_{out}^*, and a^2 are present in [26, 28, 29].

The implementation procedure of the proposed soft handoff algorithm is drawn in Figure 6(b). Note that we provide the option of dynamic channel reservation mechanism in the flowchart, in spite of its absence in our algorithm. Additionally, the exhaustive search allocation scheme incorporated in the flowchart can be traced in [30], where we proposed a modified queuing algorithm, considering that a user with a smaller required power is possible to be at the back of PQ, since the synthetic AP value is determinant when prioritizing incoming users. While in the classic first-in-first-out queuing scheme, users behind will not be allocated until all of the front users are served.

5. TRANSPORT LAYER TCP PERFORMANCE (TRANS/NET/WIRELESS LINK)

TCP congestion control is originated and well investigated in wired networks where congestion is the main cause of packet loss, thus operates properly in such networks. But wireless networks and mobile terminals feature a large amount of losses due to bit errors and handoffs, thus are in some facets non-cooperative with traditional TCP congestion control, resulting in end-to-end performance degradation. In wired networks, TCP assumes that packet loss is caused by congestions and reacts to it by decreasing the congestion window (cwnd), retransmitting the missing packets, triggering congestion control/avoidance mechanism (i.e., slow start [31]), and recalculating the retransmission timer with some backoff according to Karn's algorithm [32]. In wireless networks, when packet loss occurs for some reasons other than congestion, such as temporary blackout due to fading, or when packets are correctly received but the corresponding ACKs have not been returned which is the so-called spurious timeout, TCP will perform the same as for reacting to congestion in wired networks because it is not able to identify these different types of losses. The spurious timeouts of TCP in wireless communications eventually lead to unnecessary cwnd/throughput drop and inefficient bandwidth utilization, especially in the presence of the well-known stochastic internals of wireless scheduling which is the focus of this section. We address this problem, present existing solutions, and provide our algorithm.

Although there are difficulties implementing TCP in wireless networks, so far no single research has proposed to replace TCP with another transport layer protocol suitable for communications over wireless links. It is unwise to remove TCP since its hierarchical relationship with popular application-layer protocols such as HTTP, FTP, TELNET, and SMTP has been well established. In order to facilitate the seamless integration of mobile communications through wireless networks with the wired Internet backbone, TCP over wireless techniques are proposed. In general, the proposals found in the literature can be categorized into three classes: split-connection protocols (i.e., indirect-TCP (I-TCP) [33]), end-to-end protocols (i.e., explicit congestion notification (ECN) [34]), and link-layer proposals (i.e., forward error correction (FEC) [35]). One may refer to [36] for a detailed survey on different classifications of TCP-over-wireless solutions.

To the best of our knowledge, the impact of downlink scheduling on the performance degradation of TCP in CDMA networks has not received much research attention. Two works regarding similar issues in time-slotted networks have been found in the existing literature. Authors of [37] proposed a reservoir mechanism at the base station to store some ACKs during scheduling midseason and release them in the offseason to avoid spurious timeouts at TCP sources. It is a revised version or addition of the Snoop protocol [38] (a special link-layer protocol). The problem of this algorithm is that they use ICMP packets to measure the round trip time (RTT) for ACK release interval calculation. These extra ICMP packets can significantly increase the network traffic especially in a large network where there are lots of TCP senders and receivers. In addition, they did not demonstrate clearly what methodology they utilized to measure the idle period and the scheduling cycle at the base station. Authors of [39] proposed to use pure MAC layer information to calculate a TCP-related metric for link-layer scheduling. Thus TCP performance is maintained when they use this metric in the link layer to schedule traffic from TCP sources. This algorithm can also be called TCP-aware link-layer algorithm. A crucial part of this algorithm is to use MAC information to approximately calculate the average RTT. However, this approach is very complicated since it requires heavy mathematical calculations to obtain the new metric at the beginning of

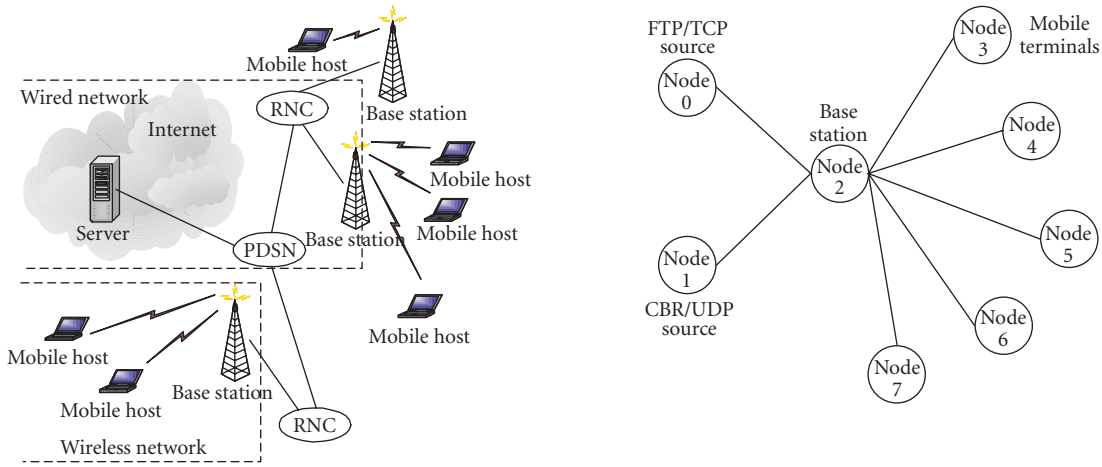

(a) The integrated network topology for TCP proposal

(b) Network topology for TCP-over-wireless simulations

Figure 7: Network topologies for TCP proposal and simulations.

each scheduling cycle and updating of the information for recursive calculation afterwards.

One of the innovations of our works is that we propose an algorithm to eliminate TCP performance degradation due to wireless scheduling in CDMA downlinks. In this paper, we do not give details on how wireless opportunistic scheduling impacts TCP performance since it is well illustrated in [37, 39]. We assume it is the existent problem and are concerned with the solutions in a CDMA environment. As addressed in the preceding section that in CDMA downlinks, scheduling users under better channel condition first can improve overall network performances. Wherever scheduling arises in wireless networks, there are impacts on TCP sources. The proposal is based on an example of real-time video transmissions where the jitter is smoothed out at the receiver to ensure a constant rate playout. We apply this idea to CDMA downlink scheduling which introduces stochastic halt affecting TCP performance at the sender (typically a fixed station in the wired part of the network from which data can be downloaded using HTTP or FTP application protocols). Figure 7(a) depicts the network topology we are dealing with, where RNC (radio network controller) and PDSN (packet data serving node) connect the wireless network with the Internet backbone.

TCP mechanism is quite mature in wired networks. The problem that we are facing now is because of the exclusion of potential wireless applications when TCP was proposed. Naturally, one solution would be emulating the behavior of the wired network, so that the "wireless" effect on TCP could be eliminated. Wired scheduling is periodical and hence predictable since every user is equal in terms of channel condition (no time-varying fading over wired links). It can be prevented and will not be a cause of TCP spurious timeouts. Thus wired scheduling is not within the scope of our study. On the other hand, wireless scheduling is unpredictable and thus irregular due to time-varying wireless links (users have to be rescheduled according to their instant channel fading). Wireless CDMA networks consist of two parts: the uplink and the downlink. In the reverse direction (uplink, i.e., from the mobile station to the base station), the key restriction is the incremental interference in the system as communicating mobiles increase, due to transmission power levels of other active users and imperfect orthogonality of channel codes. Scheduling in this direction is not needed as long as the system interference stays below the threshold. Here we assume that the simultaneously active users in the system are not enough to cause the interference beyond the threshold. Therefore, scheduling in this direction is of little importance to be considered by TCP performance. Rather, we focus on the downlink direction where we proposed novel scheduling schemes and explained their necessity and effectiveness.

Through the analysis above, downlink scheduling is the only affecting factor to degrade TCP performance in our study. Specifically, when interscheduling cutoffs (intervals/halts) occur, there is a temporary silent period in the wireless part of the network for the scheduler to collect the up-to-date channel information and to perform the new scheduling at the base station. During this period, no traffic is in the wireless network and the mobile station will not send back the expected ACK since it has not received the TCP packet queued at the base station. Consequently, the TCP source may undergo spurious timeouts without the ACK it is expecting.

What if we avoid this burst-and-silence traffic pattern to smooth the traffic throughout the burst and the following silence period, just as what we do to avoid annoying jitter in video playout? Then the TCP packets stored in the base station will arrive at the mobile station with steady rate and the mobile station will return the ACK without huge gaps for TCP to timeout. After the scheduler determines the order of the packets to be transmitted based on the channel conditions of each mobile user, it calculates a new transmission rate to send the packets in a steady pace instead of sending them out all at once. In this case, there is traffic flowing in the

Table 1: Key technical specifications of WCDMA.

Multiple access technique	Direct-spread code division multiple access	Number of slots/frame	15
Frequency reuse	1	Number of chips/slot	2560
Carrier bandwidth	4.4–5.2 MHz	Intrasystem handoff	Soft/softer handoff
Chip rate of spreading bits	3.84 Mcps	Power control period	Time slot = 1500 Hz rate
Maximum user data rate	2.3 Mbps	Power control step size	0.5, 1, 1.5, 2 dB (variable)
Frame length	10 ms (38400 chips)	Physical layer spreading factors	$4 \cdots 256$ (uplink) $4 \cdots 512$ (downlink)

network at all times so that there is no cutoff any more. This is our Proposal 1. Let the queues at the base station be per-TCP-flow and the ACK per-packet based (TCP Reno [40]). Let N_i be the number of TCP packets in queue i of the reference base station, let T_{bi} and T_{si} (in seconds) be the midseason (burst) and offseason (silence) duration of the scheduling cycle of queue i, respectively. The playout rate to smooth out the "jitter" of the burst traffic R_p is written as

$$R_p = \frac{N_i}{T_{bi} + T_{si}}, \tag{12}$$

where N_i is known to the base station through queue monitoring, $T_{bi} + T_{si}$ is equivalent to one term T_{ci}, the scheduling cycle of queue i, which can be obtained from the history as

$$T_{ci}(n) = (1 - \rho)\overline{T}_{ci}(n-1) + \rho T_{ci}(n-1), \tag{13}$$

where $T_{ci}(n)$ and $T_{ci}(n-1)$ denote the nth and its previous, the $(n-1)$th, scheduling cycles, respectively. $\overline{T}_{ci}(n-1)$ denotes the average duration of scheduling cycle of queue i up to scheduling cycle $(n-1)$. ρ is a weighing parameter with a typical value of 1/1000 [39]. The initial value of the scheduling cycle (i.e., $T_{ci}(1)$) can be monitored by the base station through some timer setting. Having smoothed out the "jitter" using the above algorithm, the base station can "play" the traffic continuously and get the ACK back to the TCP sender accordingly, without temporary blackout which is the root of TCP spurious timeout and performance degradation.

The above proposal can be easily implemented and effective, which is based on the fact that the ACK flow back to the TCP source is continuous as long as the TCP packets waiting at the base station get transmitted to the mobile destination continuously. It applies to wireless part of the network with both comparable and negligible delay compared with the delay in wired part of the network, because the timeout interval is updated by TCP through the measured variable round trip delay.

6. PERFORMANCE ANALYSIS-SIMULATION ENVIRONMENT & NUMERICAL RESULTS

We address the performance measure and numerical results in this section. As argued before (see Section 1), different interpretation of "cross-layer" yields a different concern on complex connections among layers. Some layers may interact in terms of one measure while others may be related in terms of another. In general, it is difficult to generate a method that conforms the performance measures across all the four layers involved in our research, as proposed in Sections 3–5; the interacting layers are LINK/PHY, NETWORK/LINK/PHY, and TRANSPORT/NETWORK/LINK, respectively, where they are associated based on currently prevalent and practical problems concerned. Thus for each combination which is formulated by these layers' featured relationships/interactions, there are individual measures that best exhibited the performance gain over noncombination. This is how we design the simulation senarios to exploit the performance gain for each cross-layer combination.

The simulations of the following subsections are set up in a WCDMA environment. Some of the key technical specifications of WCDMA [41] used for our simulation environment setup are listed in Table 1.

6.1. MAPQ and UF

Other relevant parameters are 19 wrap-around cells with radius $r = 500$ m (macrocell). One BS is located in the center of each cell with $P_T = 20$ W and a portion of 70% of P_T is dedicated to traffic channel [42]. Mobility speed in Rayleigh-fading model is 10 km/h (vehicular environment), $\alpha = 4$, $\sigma_X = 8$ dB, $\sigma_Y = 2$ dB, $\gamma^*_{\text{voice}} = 5$ dB, and $\gamma^*_{\text{data}} = 3$ dB.

Hybrid voice and data users are uniformly distributed, approximately 30 users per cell on average. Voice traffic is modeled as "ON-OFF" with 50% "ON" duration probability, and best-effort data traffic is generated with exponentially distributed arrival rate. Generally speaking, voice traffic has lower transmission rate compared to data traffic. In the integrated voice/data scheduling scheme, minimum voice rate R_v is selected from one of the following values: {8, 16, 32, 64} kbps corresponding to a spreading gain of 512, 256, 128, and 64, respectively, while $R_v = 64$ kbps is the fixed transmission rate in the voice-only scheduling (MAPQ). Data rate R_d can be chosen from any available value allowed by the spreading gain set of {4, 8, 16, 32, 64, 128, 256, 512}.

For voice-only scheduling, maximum tolerable delay is $d_{\max} = 100$ ms, and buffering delay ($d_b = 60$ ms) is used in

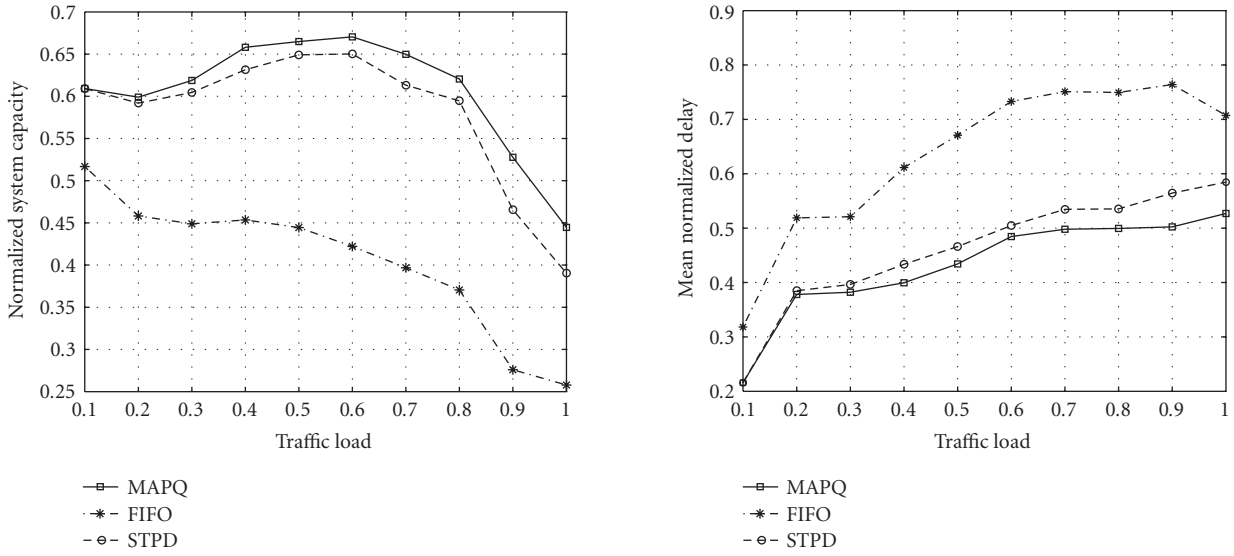

(a) System capacity comparison for MAPQ

(b) Mean normalized delay comparison for MAPQ

Figure 8: Performance evaluation of MAPQ.

the simulations to determine the unfairness criterion. The power for calculating AP is procured from (1). For integrating voice/data scheduling framework, the delay thresholds for sorting voice and data packets into different queues are $V_{\text{thre}} = 10$ ms, and $D_{\text{thre}} = 120$ ms. The delay bounds of voice and data packets are 100 ms and 2 s, respectively, which will be used in the mean normalized delay calculation in the following section.

We first define the performance measures used in the MAPQ and UF simulations for voice and data. Define N_F, N_A, N_S, N_C, ψ_F, and ψ_A as the total number of users in the network (in our case 30/cell), the number of active users in the network, the number of active users actually served, the number of cells in the system (in our case 19), the throughput (kbps) of the system if all the active users can be served, and the actual throughput of the system, respectively.

(1) MAPQ for voice only.

(i) Normalized system capacity (throughput)-ψ_A/ψ_F. Note that voice packets have constant transmission rate thus the capacity and throughput have similar behaviors.

(ii) Packet dropping probability—(number of packets dropped)/(number of packets transmitted). A voice packet is dropped if its buffering delay exceeds the delay bound (100 ms).

(iii) Unfairness probability—we call it "unfair" if a user's buffering delay is greater than d_b yet not served. Therefore, unfairness probability refers to the probability that such unfair event happens. One possible way is to use N_{UP}/N_A to measure it, where N_{UP} is the number of users that experience unfairness.

(iv) Traffic load-N_A/N_F.

(2) UF for hybrid traffic.

(i) System capacity-N_S/N_C.

(ii) Traffic throughput-ψ_A/N_C.

(iii) Outage probability: fraction of time that a user's received power is below the minimum acceptable power level to satisfy the target SIR.

(iv) Average power utilization (efficiency)—(total power consumed)/(total traffic power budget of BSs). It acts as the indicator of resource consumption efficiency.

(v) Voice ratio—the proportion of voice traffic in the hybrid traffic. It controls the variation of the hybrid traffic structure.

(3) For both MAPQ and UF.

(i) Mean normalized delay:

$$\frac{\sum_{i=1}^{N_s} (\text{normalized\_delay\_of\_packet}_i)}{N_s}, \tag{14}$$

where the numerator equals to

$$\frac{\text{buffering\_delay\_of\_packet}_i}{\text{delay\_bound\_of\_packet}_i}. \tag{15}$$

We measure the normalized delay only for successfully served users because there are other criteria, voice dropping probability and data outage, to illustrate the behavior of each scheduling scheme with service failures.

6.1.1. Voice only: MAPQ

The simulation runs over 100 000 times. Compared to systems where no sorting scheme nor modified PQ allocation

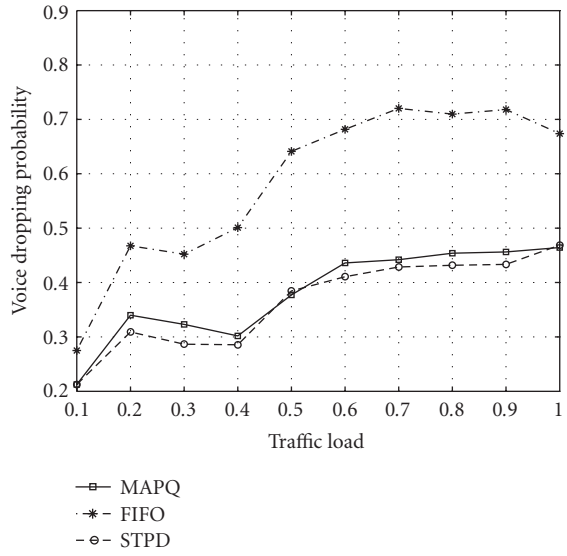

(a) Dropping probability comparison for MAPQ

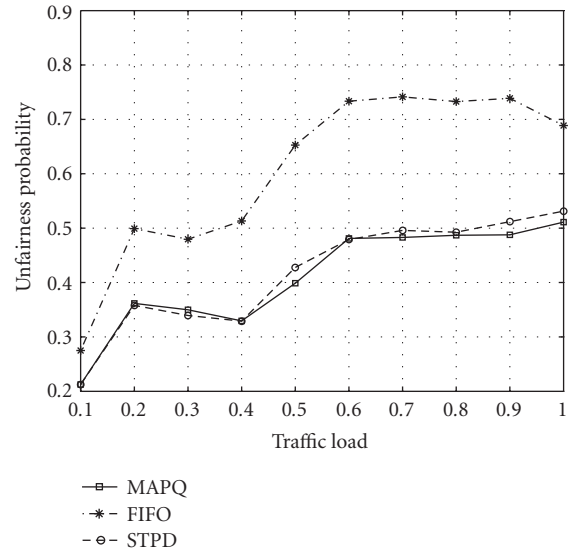

(b) Unfairness probability comparison for MAPQ

Figure 9: Performance evaluation of MAPQ.

scheme (FIFO) is deployed, system performances of the MAPQ scheme in terms of system capacity, voice packet dropping probability, mean normalized delay, and unfairness probability improve in various degrees, as shown in Figures 8 and 9, respectively.

As the traffic load grows heavier, the performance gain of the proposed scheme becomes more apparent. This can be explained by the following observations. When the power budget is getting tighter and users are more competitive for limited resources, the FIFO scheme is not capable of producing satisfactory results due to its inadaptability to severe system environment. While the MAPQ scheme is generally stable and insensitive to throughout traffic variation, and able to produce acceptable outcomes even if experiencing stringent conditions, as a result of well designed adaptive features.

Moreover, we compare the MAPQ scheme with a more advanced scheduling scheme in the literature named STPD (scheduling with transmission power and delay) [15]. In this scheme, packets whose required transmission power is less than a threshold P_{th} are classified into Group 1, otherwise are classified into Group 2. For real-time traffic like voice, if the maximum buffering delay of Group 1 is less than a delay threshold, Group 2 is transmitted first to avoid the exceeding of the tight delay bound. While for non-real-time traffic like data, Group 1 is always transmitted first since it is delay-tolerable. This algorithm is less complex in calculation since it does not use the priority to sort each packet. However, the simplicity may result in some degradation of the performance, as shown in Figures 8(a) and 8(b), where obviously the more complex MAPQ scheme performs better in terms of both the system capacity and the mean normalized delay in the network.

The MAPQ scheme not only outperforms the STPD in these criteria, but also maintains other performances in terms of voice dropping probability and unfairness probability, as shown in Figures 9(a) and 9(b). In Figure 9(b), MAPQ and STPD almost have the same performance but as the traffic load becomes heavier, the MAPQ shows the trend to outperform the STPD.

Note that the fairness criterion in our simulation is implied by both the mean normalized delay and the unfairness probability measures. Smaller normalized delay and lower unfairness probability indicate higher degree of fairness.

We also testified the necessity of both sorting and the allocation subschemes of MAPQ scheme by comparing MAPQ with two reference cases, namely, allocation (modified PQ) without sorting and sorting without allocation (classic PQ). The proposed scheme outperforms both of the references in terms of system throughput, packet dropping probability, and unfairness probability with 2%–10% performance gains (not shown in this work).

6.1.2. *Unified voice/data framework (UF)*

Individual performance gain of voice under the proposed scheduling algorithm has been procured and illustrated above in terms of system capacity/throughput, packet dropping probability, and unfairness probability. Note that the values of a, b, and c used in the simulation are obtained from the estimation.

In this section, we focus on measurable performance of hybrid voice/data traffic under the proposed unified framework. Three reference algorithms are compared with our algorithm, and evaluation is realized through several significant criteria: system capacity, traffic throughput, outage probability, average power utilization, and mean normalized delay. the first reference algorithm employs SPS (static priority scheduling) [18] algorithm for either class, the second reference algorithm employs STPD (scheduling with

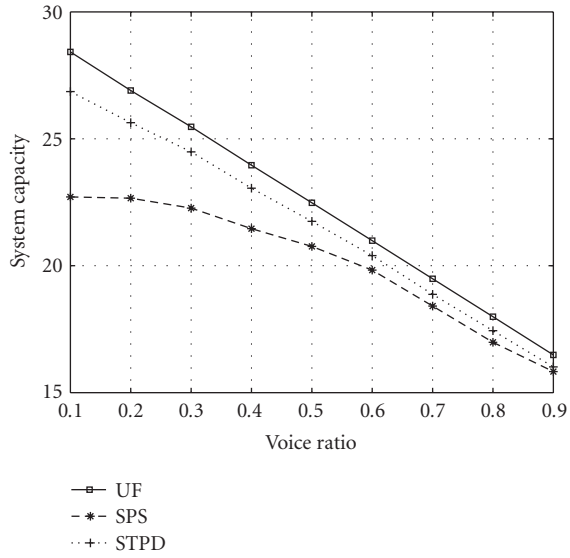

(a) System capacity comparison for UF

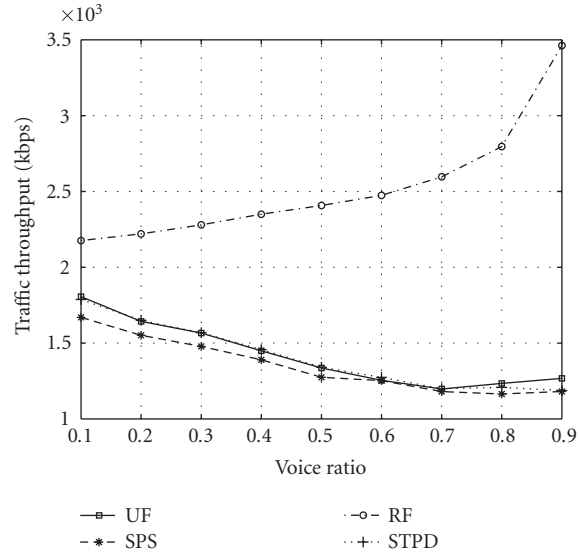

(b) Traffic throughput comparison for UF

Figure 10: Performance evaluation of UF.

transmission power and delay), and the third reference algorithm employs data scheduling only, which is the popular RF (rate fairness) algorithm as in [43, 44]. They represent three typical simulation conditions.

Figures 10 and 11 show the comparison results in terms of system capacity, traffic throughput, outage probability, power utilization efficiency, and mean normalized delay, respectively. The results are obtained by averaging over different load situations. The proposed algorithm achieves better performance in all cases in comparison with SPS and STPD. The proposed framework illustrates an appropriate combination of individual performance sustentation as well as integrated optimization and robustness. Figure 10(a) exhibits the capability of the proposed algorithm to explore the bursty nature of the data traffic with a visible steep slope of the solid square-marked curve under the variation of traffic ratio. This capability benefits from discrepancy of voice/data scheduling (i.e., different adaptive priority profiles, data reallocation mechanism) in the framework. While SPS (dashed asterisk-marked curve) appears mildest under the traffic structure change, as a result of limited capacity and resource utilization capability. Solid square-marked curves of Figures 10(a) and 10(b) confirm the results in [45] in which system throughput (Figure 10(b)) decreases with the reduction of data portion, probably because of the fact that data traffic has much more burst and much higher bit rate, thus is more susceptible to load change and affects more on throughput and capacity (Figure 10(a)) behaviors.

Although RF has much higher traffic throughput (observed in Figure 10(b), circle-marked dash-dot curve) because it distributes rate equally among all active users regardless of actual channel impairments, which comes at the expense of users being served with power below the minimum acceptable target at most of the time (circle-marked dash-dot curve in Figure 11(a)), this insufficient transmission power fails to combat channel fading and causes transmission failure (SIR target unsatisfied). While the power baseline in SPS is assured, because of the lack of sorting process, users are served in a first-in-first-out mode where a user occupying large power is possible to be allocated before users requesting smaller power. Also, due to our allocation subalgorithm which is based on an exhaustive search mechanism, system capacity and traffic throughput of the proposed algorithm outperform those of SPS as displayed in Figures 10(a), 10(b) (solid versus dashed curves), respectively, without sacrificing QoS satisfaction degree (here defined by outage probability as in Figure 11(a), solid versus dashed curve).

Aside from the exploitation and maintenance of individual behavior features, the capability of attaining overall optimization and robustness to various traffic structure, resulting from the consistent infrastructure of the framework, is depicted in Figures 11(a), 11(b), and 11(c), since in these figures the fluctuation of the traffic structure does not affect UF much.

Voice traffic has less burst, smaller range, and lower data rate than data traffic. Wang et al. [19] advocates that with the same total offered load, a larger fraction of voice permits better multiplexing and hence more efficient resource usage, giving rise to the fluctuation of average power utility with voice ratio, shown in their simulation results. On the contrary, Figure 11(b) convincingly illustrates that the UF guarantees power utilization efficiency at above 97% at all times benefiting from data reallocation mechanism and is resistible to a variety of offered traffic load and voice/data ratio. At the same time, the obvious fluctuation of the dashed curve and the dotted curve reflects the vulnerability of SPS and STPD under the altered traffic structure.

Further, the reallocation mechanism ensures "good" users to be better and "poor" users to be served, leading to fairness protection as shown in Figure 11(c), low and

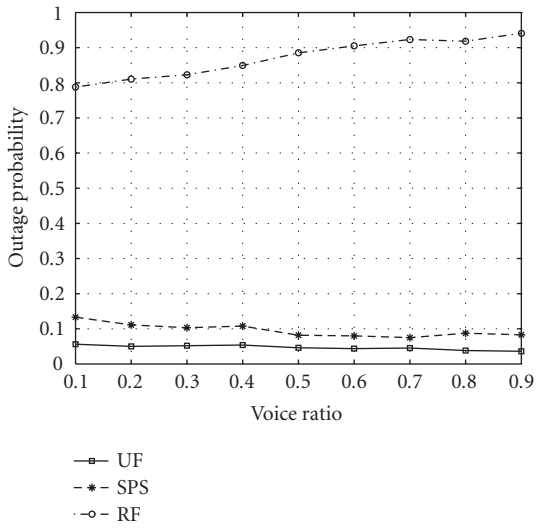

(a) Outage probability comparison for UF

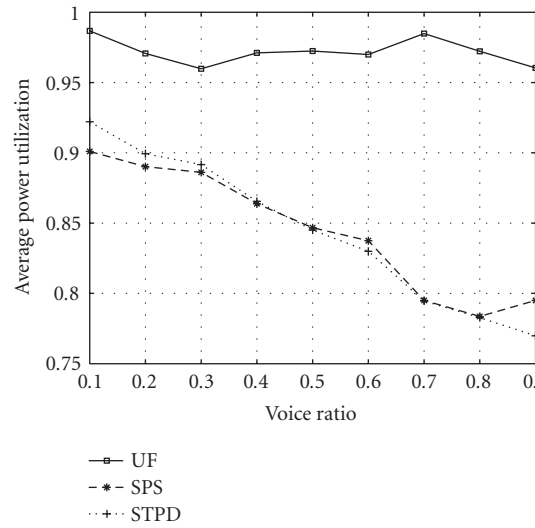

(b) Power utilization efficiency evaluation for UF

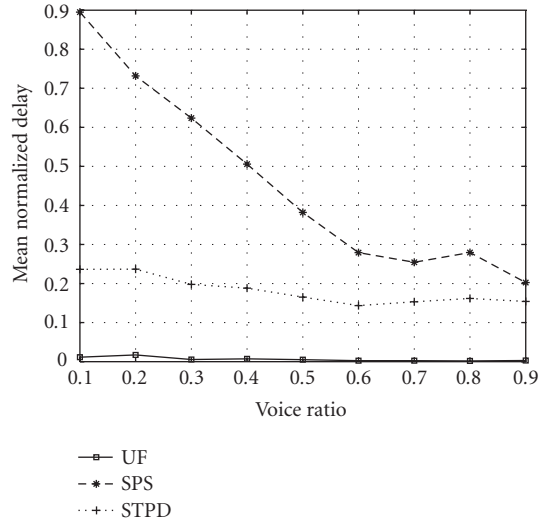

(c) Mean normalized delay (fairness) evaluation for UF

Figure 11: Performance evaluation of UF.

insensitive outage occurrence (solid curve in Figure 11(a), reflecting high degree of QoS satisfaction) throughout varied voice ratio.

Figure 11(c) shows the outstanding delay performance of the UF scheme. In general, higher voice ratio yields better delay performance since data packets may experience much longer delay thus have larger impact on the delay behavior in the network. In fact, the delay behavior of the MAPQ scheme in Figure 8(b) does not show such striking performance enhancement. We mentioned before that data packet delay is usually much larger than voice packet delay. The data packet delay performance determines the delay performance of the entire network. Therefore, we can conclude that the result in Figure 11(c) suggests that the gain of the UF scheme comes largely from the desirable delay performance of data users. Due to the dominant characteristics of data packet delay in the network, this performance gain also compensates for the voice packet delay performance, observed as a nearly flat curve (the solid square-marked curve) in Figure 11(c). This nonfluctuated delay performance curve further demonstrates the fairness assurance among data users in the UF scheme. In addition, it implies that, in the MAPQ scheme, the improved performance of voice packets does not necessarily sacrifice the data packets behavior (i.e., data packet delay).

We believe all of the above gains are acquired from the unity of proposed framework and innovative sorting and allocation (reallocation) mechanisms deployed within.

Table 2: Simulation parameters of the proposed handoff algorithm.

System parameters	Value	Handoff parameters	Value
Bandwidth/chiprate	5 MHz/3.84 Mcps	AS_Th/AS_Hyst/ΔT	2 dB/2 dB/0
Cell radius	1000 m (macrocell)	W_t, D_{th}	1 s, 2 min
User locations/arrival type	Uniformly/exp. distributed	T_c (exp. distributed)	Mean 1 min
P_T, P_t	20 W, 70% P_T	P_G (for each neighbor)	4% P_t
Traffic model	ON-OFF, 50% ON Prob.	λ, μ	0.85, 0.8
User mobility/max speed	2-dimen. Rand. walk/100 Km/h	a^2	0.5
R_v set	$\{64, 32, 16, 8\}$ kbps	Max. γ_d	6.2 dB
$\alpha/\sigma_X/\gamma^*$	4/8 dB/5 dB	P^*_{out}	0.1

6.2. Prioritizing handoff algorithm

Next, the performance of the network layer proposal is evaluated. Table 2 displays the system and handoff parameters for our simulation senario. Handoff parameters such as $W_t/\lambda/P_G$, μ (derived from normalized R_s, the radius of nonsoft handoff zone in [46]), and $a^2/\gamma_d/P^*_{\text{out}}$ are obtained from [19, 28, 46], respectively. In [19], a fixed guard capacity reservation scheme is shown to have similar performance to their dynamic ones in terms of new call blocking probability, handoff dropping probability, and average power utilization but with higher guard power waste at lighter load. Therefore, we employ fixed reservation scheme for simplicity and generate heavier traffic load (50%–100%) to diminish the guard power utilization discrepancy. Offered traffic load used in the following figures is the actual amount of traffic normalized by the fully loaded amount of traffic in the network. Heavier traffic load imposes greater challenge on the success of the proposed algorithm because of more severe dropping condition.

Figures 12(a)–12(c) demonstrate that the proposed prioritizing algorithm outperforms the FG (fixed guard capacity) scheme [19] in terms of handoff dropping probability (P_d), average guard power efficiency, and average guard power utilization, under the same prediction scheme and general handoff procedure proposed in Section 4.3. These performance measures are defined below, where N_{tho}, N_d, N_{ssho}, $P_{\text{rsv grd}}$, and $P_{\text{sum ho}}$ denote total number of received handoff calls, the number of blocked (dropped) handoff calls, the number of successful handoff users, total reserved guard power, and total consumed guard power (sum of successful handoff powers derived from (10)), respectively.

(i) P_d-N_d/N_{tho}.

(ii) The guard power efficiency-$N_{\text{ssho}}/P_{\text{rsv grd}}$. It indicates the number of successful handoff users that can be supported by consuming certain $P_{\text{rsv grd}}$, thus clarifies the efficiency of $P_{\text{rsv grd}}$.

(iii) The guard power utilization-$P_{\text{sum ho}}/P_{\text{rsv grd}}$. It indicates the utility of the reserved guard power. If it is too low, that implies the underutilization and a waste of system resources.

We run over 10 000 trials and get the averages of the above performance indicators as seen in Figures 12(a), 12(b), and 12(c).

The reason for the outperformance has two folds which reflect the innovation of the proposed prioritizing algorithm. (1) Handoff users demanding smaller powers are scheduled first in general, contributing to a larger number of successful handoff users with the same amount of guard power, thus P_d is reduced (Figure 12(a)) and power efficiency is enhanced (Figure 12(b)).

(2) Handoff users who have been connected for a longer call time ($T_c < D_{\text{th}}$) are more likely to cease and release resources shortly, before other concurrent handoffs are dropped due to the lack of enough guard resources. It can be interpreted as the resource borrowing (or reuse) mechanism of earlier and faster handoffs from slower handoffs, giving rise to higher guard power utilization (Figure 12(c)).

Note that an overlow λ triggers more frequent and false predictions, because it extends the active set and may lead to too weak potential BSs. While an overhigh one hinders potential true predictions. Consequently, this parameter has to be designed carefully. The authors [19] addressed similar concerns on λ. We use $\lambda = 0.85$ as indicated in [19].

From Figures 12(b) and 12(c) we observe that higher offered load yields larger difference between the proposed algorithm and the FG. Indeed, whether the guard capacity reservation scheme is fixed or adaptive produces no distinction in terms of average guard power utilization, as shown in [19]. However, the fixed and adaptive reservation schemes can affect the handoff dropping probability to have very different performances, which is verified also in the above research work. Additionally, the authors show that the adaptive reservation schemes exhibit greater difference between each other as the offered traffic load grows. But since we employ fixed reservation schemes, the fixed guard power may fail to exploit or adapt to the dynamics of the handoff dropping probability when the system is highly loaded and has poorer dropping behavior. This explains the reason for the nearly parallel curves in Figure 12(a). In the future research, more performance gains of dropping probability are expected with the employment of the adaptive guard capacity reservation scheme in the proposed handoff algorithm.

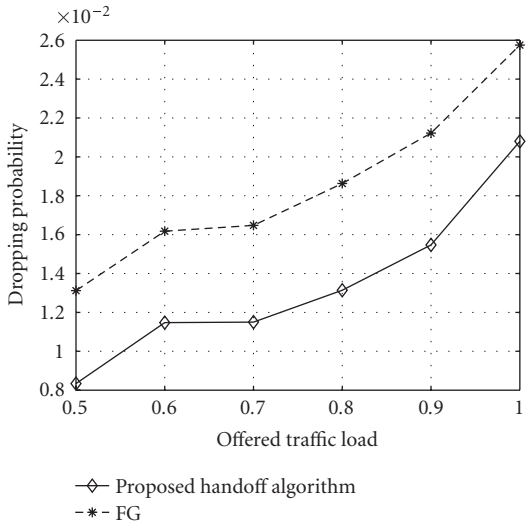

(a) Handoff dropping probability

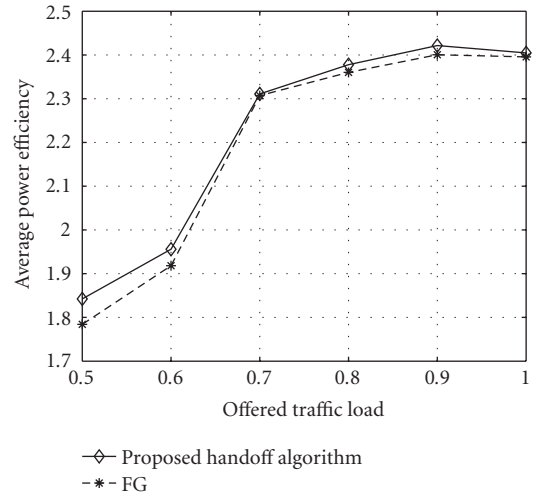

(b) Average power efficiency for handoff algorithm

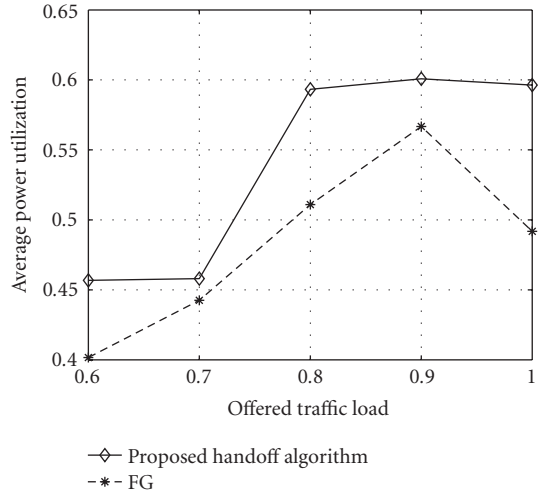

(c) Average power utilization for handoff algorithm

Figure 12: Performance evaluation of the proposed handoff algorithm.

6.3. TCP cwnd behaviors

Finally, the performance analysis of transport-layer TCP/wireless is presented. This section is dedicated to the numerical results for the feasibility of the proposed algorithm (Proposal 1) for TCP performance improvement, in terms of the evolution of TCP congestion window (cwnd) and TCP throughput. With the reasonable analysis and implementation details, success and effectiveness of the proposed algorithm is further confirmed in the simulation. While the network simulator-version 2 (NS-2) [47] models do not support CDMA air interface or CDMA MAC implementations, there is difficulty to simulate the TCP performance with the presence of the proposed scheduling schemes in NS-2. In this paper, we provide the experimental results using MATLAB and leave the simulations in NS-2 for future work. We set up a simple network as shown in Figure 7(b), where there are a FTP source (node 0) sending TCP (data) traffic and a CBR source (node 1) sending UDP (voice/video, referred to as voice hereafter for simplicity) traffic. We create 5 nodes (nodes 3–7) at the wireless terminal as the receivers of both TCP and UDP packets. The base station is modeled by node 2 connecting the bottleneck link. Note that the simulation for Proposal 1 does not include the UDP sender thus studies the TCP performance based on a pure TCP-traffic network. However, the simulation for the extended analysis of the design parameters employs exactly the topology as Figure 7(b).

The MSs act as the TCP sinks. Assume that the TCP sender always has data to transmit and can transmit as many packets as its transmission window allows (bulk TCP data). The TCP sinks receive TCP packets to deliver them to the user and generate immediate ACKs for the TCP sender. The TCP mechanism implemented for the experiment is only related

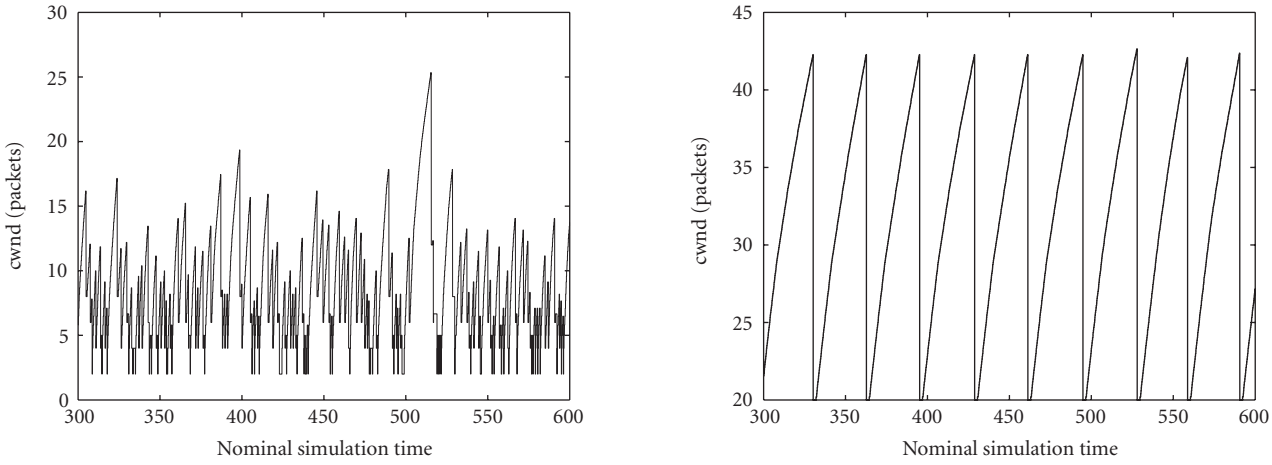

(a) Evolution of TCP cwnd for standard TCP

(b) Evolution of TCP cwnd for Proposal 1

Figure 13: Performance evaluation for TCP cwnd behaviors.

to dynamic congestion window evolution, according to the slow start and congestion avoidance algorithms [31]. Other mechanisms such as retransmission and recovery for error control are not considered.

The data is transmitted using variable bit rate in the TCP packets with a length of 1000 bytes/packet. Voice (only simulated later in the extended analysis for design parameters analysis) is transmitted in the UDP packet with constant bit rate selected from one of the following values: 8 kbps, 16 kbps, 32 kbps, and 64 kbps, as used in the scheduling schemes in Section 3. The packet length of a UDP packet is a design parameter in our research and will be demonstrated later. The buffers proposed in the base station and the TCP sender are per-TCP-connection and drop-tail, with the size varied in the simulation. The bandwidth and propagation delay of the wired connections (node 0-node 2, node 1-node 2) are 20 Mbps and 20 ms, while they are set to 1 Mbps and 1 ms for the wireless connections (node 2-node i, $i = 3, 4, 5, 6, 7$).

Since the scheduling cycle and interscheduling cutoff parameters vary depending on the complexity and execution time of different scheduling schemes, no typical parameters are found in the literature. In reality, wireless service providers deploy real-time monitoring systems to obtain useful statistics such as link activity, bandwidth utilization, link occupation time, throughput, for internal and external uses. Link activity makes the scheduling cycle easy to be measured because the link will be idle if interscheduling cutoff happens. In our simulation, NS-2 provides real-time monitoring mechanisms such as queue-monitor by which we can measure the scheduling cycle using the packet arrival-departure statistics in the queue-monitor output. Interscheduling cutoff happens at 0 departures.

6.3.1. Proposed TCP algorithm

The congestion window behavior of Proposal 1 is compared to that of the standard TCP, TCP Reno [40] with standard ACK (one ACK per TCP packet). The design parameter chosen for this purpose is the buffer size/queue limit BU. We set it to 40 (packets) based on the analysis in the extended simulations. Figures 13(a) and 13(b) illustrate the evolution of cwnd in terms of the nominal simulation time, for standard TCP and Proposal 1, respectively. Note that the nominal simulation time is used as the x-axis instead of the real simulation time (s) because of the lack of the simulator. We run the simulation created by algorithms in MATLAB for over 60 000 times, approximately every 10 000 times represents a 100 s in a real simulator (i.e., NS-2). The curves in Figures 13(a) and 13(b) are plotted using the data obtained from every nominal time (0.01 s in NS-2).

In order to distinguish the spurious timeout and the real-loss-triggered timeout, we set the wireless link loss (due to shadowing and fading) to be 0. The irregular fluctuation of the cwnd in Figure 13(a) suggests only the spurious timeout due to wireless scheduling intervals and implies the incompetence of the standard TCP in the presence of wireless scheduling, which is implemented based on the MAPQ and the UF schemes proposed in Section 3. We also observe from Figure 13(b) that, compared to standard TCP, Proposal 1 performs much better in the cwnd evolution because it avoids the spurious timeouts which largely degrade the cwnd performance. We acquire the desired cwnd behavior from Figure 13(b) that the congestion window keeps increasing until the buffer overflows. Thus, the maximum window size is always maintained which is approximate to the buffer size (in our simulation 40 packets). While the congestion window behavior in Figure 13(a) does not obey the sawtooth shape, and the achievable window size is even less than 20.

In addition, we analyze the TCP throughput performance for the standard TCP and Proposal 1, as displayed in Table 3. The throughput is calculated by

$$\text{Thru}_{\text{TCP}} = L_{\text{TCP}} N_{\text{TCP}} / T_{\text{nom}}, \tag{16}$$

where Thru_{TCP}, L_{TCP}, and N_{TCP} denote the TCP throughput (bps), the TCP packet length (8000 bits/packet), and the

Table 3: TCP throughput comparison.

TCP scheme	Throughput (kbps)	Number of TCP packets generated
Standard	54.216	89149
Proposal 1	70.217	90125

Table 4: Effects of design parameters on TCP cwnd behavior.

$PS_{(CBRR=64,BU=30)}$	Achievable cwnd	$CBRR_{(PS=80,BU=30)}$	Achievable cwnd	$BU_{(PS=80,CBRR=64)}$	Achievable cwnd
80	5.9	8	20.5	20	3.9
200	7.7	16	14	200	11.2
1000	16.8	32	8.2	400	21.1

total number of TCP packets generated (shown in Table 3), respectively. T_{nom} denotes the total nominal simulation time.

We may not see striking throughput gain from this example since the network we built is relatively simple thus not enough traffic is generated to test the throughput behavior. But from the tendency one can clearly tell that Proposal 1 has more desirable throughput performance than the standard TCP. We believe that with heavy loaded network simulated in the future, this throughput gain will be more apparent.

6.3.2. Extended analysis of the design parameters

Although the impacts of the network layer QoS profile, which manages the queuing disciplines and the bandwidth allocation, are beyond the scope of this research, we analyze the basic role in the evolution of TCP congestion window since the queuing mechanism for Proposal 1 at the base station makes use of the network layer functions. We found through the simulation by using NS-2 that, in general, the variations of PS (voice packet size), CBRR (voice transmission rate), and BU have great impacts on TCP cwnd. In the subsequent simulations, we employ standard TCP over the wired network (topology shown in Figure 7(b)) with 0 loss rate to study the effects of the design parameters. Table 4 illustrates the change of cwnd as a result of the varying PS (in the simulation 80, 200, and 1000 bytes) with CBRR fixed at 64 kbps and BU 30 packets; the varying CBRR (8, 16, and 32) with fixed PS and BU at 80 and 30, respectively; the varying BU (20, 200, and 400) with fixed PS 80 and fixed CBRR 64.

It is noticed that a smaller PS results in greater reduction of congestion window size, which will largely affect the improvement of TCP throughput. The reason maybe that since the wired links in the network have the same bandwidth, the smaller voice packets produced by the CBR source arrive faster and have a higher generation rate. They are of higher probability to be queued in front of the bigger data packets thus get transmitted first. On the other hand, data packets are more likely to be dropped if the queue overflows. This loss of TCP packets will further lead to the loss of the corresponding ACK. It will eventually triggers the TCP timeout and then the congestion window reduction. Note that we did not configure queuing-related parameters (e.g., queuing disciplines) since they are not considered in this research. By default the queue is FIFO and drop-tail.

The CBRR impacts present the rationale explicitly: the higher the voice transmission rate is, the more likely that there is congestion in the network since the bandwidth resource becomes more demanding. The increasing contention for the available bandwidth will induce more packet loss for both traffic, and the timeouts will occur inevitably which decreases the congestion window size.

It makes sense from the BU effects that if the buffer is designed to be small, the memory required for buffering is low trading off the maximum attainable cwnd because the buffer will be full rapidly. In other words, optimizing the congestion window with a large buffer challenges the excessive memory which can be costly. The buffer selection is hence important as well as complicated and should be designed carefully. Furthermore, we realize through the comparison of 16 kbps CBRR and 200 packets BU that a lower transmission rate (16 kbps versus 64 kbps) requires a considerably smaller buffer (30 versus 200), yielding similar or even better cwnd performance. Analysis of the buffer size is the only issue involved as the network-layer mechanism that we address in this work. Taking the comparison and analysis of this subsection into account, we designed the simulation parameter BU in the earlier simulation.

From the extended analysis of the design parameters, we further conclude that for an algorithm or a protocol to work appropriately, several key parameters (i.e., PS, CBRR, BU) need to be tuned carefully.

The experiment and simulation for this subsection are primarily operated for verifying the feasibility and effectiveness of the proposed strategies. It is preparatory for our future research which includes in-depth study of the impacts of varying TCP/UDP traffic ratio on TCP behaviors in the integrated wired/wireless environment which were somehow demonstrated in the above simulations; a more realistic network structure and traffic generation for overcoming practical problems, such as the existent "wireless" effect on TCP performance, using NS-2.

7. CONCLUSIONS AND OPEN ISSUES

In this work, we analyzed and designed cross-layer algorithms/schemes to improve overall performance across the entire cellular CDMA network, specialized in downlinks. We proposed a link-layer scheduling scheme MAPQ as a cross-layer resource management issue for efficient resource allocation of underlying layer. Evaluation of the proposed scheme has been performed with a reference scheme and superiorities are verified. It should be noted that this scheme can also be used for data scheduling with slight modification of wdp (weight of delay over power) and QoS requirement of data traffic.

Considering queuing delay as an important event trigger and service indicator, together with required transmission power/rate, we also proposed an adaptive priority-based scheduling algorithm for unified voice/data frameworking and succeeded in fulfilling preset expectation through simulation.

By jointly considering downlink transmission power and call holding time, we proposed an adaptive prioritizing algorithm to control concurrent handoff events to the same destination. The performance improvement was obtained in the simulation.

At the transport layer, we studied its interaction with wireless link layer, particularly, wireless link scheduling. We proposed an algorithm to avoid TCP spurious timeouts, to regulate the behavior of TCP congestion window, and to enhance the TCP throughput. These methods are claimed to be reasonable by theoretical analysis as well as the simulation verification. Extension of the simulation network and the traffic load scale to obtain greater performance gain of the proposed strategies is left to our future work.

Note that the complexity of our scheduling algorithms is determined fully by the real-time monitoring system. The computational part of the algorithms is simple. Once the parameters involved in the algorithms are procured from real-time measuring, the rest of the work is just simple calculations. In our algorithms, power and delay are the key parameters to be obtained. The downlink transmission power for each subscriber is monitored and adjusted frequently to ensure the quality of service. The buffering delay is another important QoS measure, especially where the system resource needs to be allocated to support class-of-service. It is critical to ensure the delay bound for different classes. As mentioned above, wireless service providers are equipped with such monitoring system to make the procurement of these parameters in real time possible.

Although the results obtained are what we have expected and are encouraging, there are some open issues and limitations of this work which call for deeper investigation.

Further Considerations

(1) The performance of the unified voice/data scheduling framework was studied in a 19-cell layout. However, we can further consider the effects of the load variations in the outer cells on the performance in a target cell.

(2) In Section 3, further details pertaining to the choice of the parameters (a, b, and c) will be provided.

(3) Another aspect which is not covered in this algorithm is the additional handoff execution time caused by the introduction of the priority queuing. This can be important when signals from cells in the active set are dropping quite fast.

(4) To import dynamic or adaptive guard capacity reservation scheme to the proposed handoff prioritizing algorithm would be an interesting topic.

(5) More results will be shown on the role of λ (the design parameter that alters the prediction threshold in the proposed handoff algorithm) and the capacity of base stations.

(6) For the TCP proposals, we will build up a larger scaled network where more subscribers and application sources will be generated for deeper understanding of the TCP behaviors.

(7) In-depth study of the impacts of varying TCP/UDP traffic ratio on TCP behaviors in the integrated wired/wireless environment.

REFERENCES

[1] A. J. Goldsmith and S. B. Wicker, "Design challenges for energy-constrained ad hoc wireless networks," *IEEE Wireless Communications*, vol. 9, no. 4, pp. 8–27, 2002.

[2] L. Alonso and R. Agusti, "Automatic rate adaptation and energy-saving mechanisms based on cross-layer information for packet-switched data networks," *IEEE Communications Magazine*, vol. 42, no. 3, pp. S15–S20, 2004.

[3] F. Yu and V. Krishnamurthy, "Cross-layer QoS provisioning in packet wireless CDMA networks," in *Proceedings of IEEE International Conference on Communications (ICC '05)*, vol. 5, pp. 3354–3358, Seoul, Korea, May 2005.

[4] J. Price and T. Javidi, "Cross-layer (MAC and transport) optimal rate assignment in CDMA-based wireless broadband networks," in *Proceedings of the 38th Asilomar Conference on Signals, Systems and Computers*, vol. 1, pp. 1044–1048, Pacific Grove, Calif, USA, November 2004.

[5] V. Friderikos, L. Wang, and A. H. Aghvami, "TCP-aware power and rate adaptation in DS/CDMA networks," *IEE Proceedings: Communications*, vol. 151, no. 6, pp. 581–588, 2004.

[6] E. Hossain and V. K. Bhargava, "Cross-layer performance in cellular WCDMA/3G networks: modelling and analysis," in *Proceedings of IEEE International Symposium on Personal, Indoor and Mobile Radio Communications (PIMRC '04)*, vol. 1, pp. 437–443, Barcelona, Spain, September 2004.

[7] J. Yao, T. C. Wong, and Y. H. Chew, "Cross-layer design on the reverse and forward links capacities balancing in cellular CDMA systems," in *Proceedings of IEEE Wireless Communications and Networking Conference (WCNC '04)*, vol. 4, pp. 2004–2009, New Orleans, La, USA, March 2004.

[8] Y. S. Chan, Y. Pei, Q. Qu, and J. W. Modestino, "On cross-layer adaptivity and optimization for multimedia CDMA mobile wireless networks," in *Proceedings of the 1st IEEE-EURASIP International Symposium on Control, Communications, and Signal Processing (ISCCSP '04)*, pp. 579–582, Hammamet, Tunisia, March 2004.

[9] S. Singh, V. Krishnamurthy, and H. V. Poor, "Integrated voice/data call admission control for wireless DS-CDMA systems with fading," *IEEE Transactions on Signal Processing*, vol. 50, no. 6, pp. 1483–1495, 2002.

[10] C. Comaniciu and H. V. Poor, "Jointly optimal power and admission control for delay sensitive traffic in CDMA networks

with LMMSE receivers," *IEEE Transactions on Signal Processing*, vol. 51, no. 8, pp. 2031–2042, 2003.

[11] S. A. Ghorashi, L. Wang, F. Said, and A. H. Aghvami, "Impact of macrocell-hotspot handover on cross-layer interference in multi-layer W-CDMA networks," in *Proceedings of the 5th European Personal Mobile Communications Conference (EPMCC '03)*, pp. 580–584, Glasgow, UK, April 2003.

[12] W. C. Jakes, *Microwave Mobile Communications*, John Wiley & Sons, New York, NY, USA, 1993.

[13] M. K. Karakayali, R. Yates, and L. Razumov, "Throughput maximization on the downlink of a CDMA system," in *Proceedings of IEEE Wireless Communications and Networking Conference (WCNC '03)*, vol. 2, pp. 894–901, New Orleans, La, USA, March 2003.

[14] D. Zhao, X. Shen, and J. W. Mark, "Effect of soft handoff on packet transmissions in cellular CDMA downlinks," in *Proceedings of the International Symposium on Parallel Architectures, Algorithms and Networks (I-SPAN '04)*, pp. 42–47, Hong Kong, May 2004.

[15] D. Kitazawa, L. Chen, H. Kayama, and N. Umeda, "Downlink packet-scheduling considering transmission power and QoS in CDMA packet cellular systems," in *Proceedings of the 4th IEEE International Workshop on Mobile and Wireless Communications Network (MWCN '02)*, pp. 183–187, Stockholm, Sweden, September 2002.

[16] W.-H. Sheen, I.-K. Fu, and K. Y. Lin, "New load-based resource allocation algorithms for packet scheduling in CDMA uplink," in *Proceedings of IEEE Wireless Communications and Networking Conference (WCNC '04)*, vol. 4, pp. 2268–2273, New Orleans, La, USA, March 2004.

[17] D. M. Novakovic and M. L. Dukic, "Evolution of the power control techniques for DS-CDMA toward 3G wireless communication systems," *IEEE Communications Surveys and Tutorials*, vol. 3, no. 4, fourth quarter, pp. 2–15, 2000.

[18] J.-H. Yoon, M.-J. Sheen, and S.-C. Park, "Scheduling methods with transmit power constraint for CDMA packet services," in *Proceedings of the 57th IEEE Semiannual Vehicular Technology Conference (VTC '03)*, vol. 2, pp. 1450–1453, Jeju, Korea, April 2003.

[19] X. Wang, R. Ramjee, and H. Viswanathan, "Adaptive and predictive downlink resource management in next generation CDMA networks," in *Proceedings of the 23rd Annual Joint Conference of the IEEE Computer and Communications Societies (INFOCOM '04)*, vol. 4, pp. 2754–2765, Hong Kong, March 2004.

[20] J. W. Chang and D. K. Sung, "Adaptive channel reservation scheme for soft handoff in DS-CDMA cellular systems," *IEEE Transactions on Vehicular Technology*, vol. 50, no. 2, pp. 341–353, 2001.

[21] J. Y. Sun, L. Zhao, and A. Anpalagan, "Soft handoff prioritizing algorithm for downlink call admission control of next-generation cellular CDMA networks," in *Proceedings of 16th IEEE International Symposium on Personal, Indoor and Mobile Radio Communications (PIMRC '05)*, Berlin, Germany, September 2005.

[22] 3GPP TR 25.922 v3.6.0, "Radio resource management strategies," 2001.

[23] V. K. Garg, *IS-95 CDMA and CDMA 2000: Cellular/PCs Systems Implementation*, Prentice Hall, Englewood Cliffs, NJ, USA, 1999.

[24] A. Viterbi, *CDMA Principles of Spread Spectrum Communications*, Addison-Wesley, Reading, Mass, USA, 1995.

[25] 3GPP TS 25.331, "RRC protocol specification," 2000.

[26] D. Wong and T. J. Lim, "Soft handoffs in CDMA mobile systems," *IEEE Personal Communications*, vol. 4, no. 6, pp. 6–17, 1997.

[27] 3GPP TS 25.214, "Physical layer procedures (FDD) v3.1.0," 1999.

[28] A. Viterbi, A. M. Viterbi, K. S. Gilhousen, and E. Zehavi, "Soft handoff extends CDMA cell coverage and increases reverse link capacity," *IEEE Journal on Selected Areas in Communications*, vol. 12, no. 8, pp. 1281–1288, 1994.

[29] K. M. Rege, S. Nanda, C. F. Weaver, and W.-C. Peng, "Analysis of fade margins for soft and hard handoffs," in *Proceedings of the 6th IEEE International Symposium on Personal, Indoor and Mobile Radio Communications (PIMRC '95)*, vol. 2, pp. 829–835, Toronto, Canada, September 1995.

[30] J. Y. Sun, Y. F. Peng, and L. Zhao, "A novel packet scheduling scheme based on adaptive power/delay for efficient resource allocation in downlink CDMA systems," in *Proceedings of IEEE Canadian Conference on Electrical and Computer Engineering (CCECE '05)*, Saskatoon, Canada, May 2005.

[31] V. Jacobson, "Congestion avoidance and control," in *Proceedings of ACM SIGCOMM*, pp. 273–288, Stanford, Calif, USA, August 1988.

[32] P. Karn and C. Partridge, "Improving round-trip time estimates in reliable transport protocols," *ACM Transactions on Computer Systems*, vol. 9, no. 4, pp. 364–373, 1991.

[33] A. Bakre and B. R. Badrinath, "I-TCP: indirect TCP for mobile hosts," in *Proceedings of IEEE International Conference on Distributed Computing Systems (ICDCS '95)*, pp. 136–146, Vancouver, BC, Canada, May-June 1995.

[34] S. Floyd, "TCP and explicit congestion notification," *ACM Computer Communication Review*, vol. 24, no. 5, pp. 10–23, 1994.

[35] S. Lin and D. J. Costello, *Error Control Coding: Fundamentals and Applications*, Prentice-Hall, Englewood Cliffs, NJ, USA, 1983.

[36] H. Balakrishnan, V. N. Padmanabhan, S. Seshan, and R. H. Katz, "A comparison of mechanisms for improving TCP performance over wireless links," *IEEE/ACM Transactions on Networking*, vol. 5, no. 6, pp. 756–769, 1997.

[37] Y. Wu, Z. Niu, and J. Zheng, "A network-based solution for TCP in wireless systems with opportunistic scheduling," in *Proceedings of IEEE International Symposium on Personal, Indoor and Mobile Radio Communications (PIMRC '04)*, vol. 2, pp. 1241–1245, Barcelona, Spain, September 2004.

[38] H. Balakrishnan, S. Seshan, and R. H. Katz, "Improving reliable transport and handoff performance in cellular wireless networks," *ACM Wireless Networks*, vol. 1, no. 4, pp. 469–482, 1995.

[39] T. E. Klein, K. K. Leung, and H. Zheng, "Improved TCP performance in wireless IP networks through enhanced opportunistic scheduling algorithms," in *Proceedings of IEEE Global Telecommunications Conference (GLOBECOM '04)*, vol. 5, pp. 2744–2748, Dallas, Tex, USA, November-December 2004.

[40] W. Stevens, "TCP Slow Start, Congestion Avoidance, Fast Retransmission, and Fast Recovery Algorithms," *RFC-2001*, January 1997.

[41] "WCDMA (UMTS): FDD technical summary," http://www.umtsworld.com/technology/wcdma.htm.

[42] W.E.A 3GPP 2, "1xEV-DV evaluation methodology-addendum (v6)," 2001.

[43] F. Xu, M.-H. Ye, P. Zhao, and H.-M. Zhang, "The research on the service rate adaptation in mobile network," in *Proceedings of International Conference on Communication Technology (ICCT '03)*, vol. 2, pp. 970–976, Beijing, China, April 2003.

[44] M. Kazmi and N. Wiberg, "Power and rate assignment policies for best-effort services in WCDMA," in *Proceedings of the 13th IEEE International Symposium on Personal, Indoor and Mobile Radio Communications (PIMRC '02)*, vol. 4, pp. 1601–1605, Lisbon, Portugal, September 2002.

[45] Y. Chen and L. G. Cuthbert, "Downlink performance of different soft handover algorithms in 3G multi-service environments," in *Proceedings of the 4th IEEE International Workshop on Mobile and Wireless Communications Network (MWCN '02)*, pp. 406–410, Stockholm, Sweden, September 2002.

[46] Y. Chen and L. Cuthbert, "Optimum size of soft handover zone in power-controlled UMTS downlink systems," *IEE Electronics Letters*, vol. 38, no. 2, pp. 89–90, 2002.

[47] "The network simulator - ns-2," http://www.isi.edu/nsnam/ns.

Jin Yuan Sun received the M.A.S. degree in computer networks from Ryerson University, Canada, in 2005. She received the B.S. degree in computer information systems from Beijing Information Technology Institute, China, in 2003. Since 2005, she has been working as a Network Test Developer at RuggedCom Inc., Ontario, Canada. Her research interests are in wireless communications, computer networks, mobile networks, and sensor networks. She is a student Member of IEEE.

Lian Zhao received the Ph.D. degree in electrical and computer engineering from the University of Waterloo, Canada, in 2002. Before she joined Ryerson University in 2003, she worked as a postdoctoral fellow with the Center for Wireless Communications, University of Waterloo. Since 2003, she has been working as an Assistant Professor at the Department of Electrical and Computer Engineering, Ryerson University, Toronto, Canada. She is a cofounder of the *Optic Fiber Sensing Wireless Network Laboratory* in 2004. Her research interests are in the areas of wireless communications, radio resource management, power control, as well as design and applications of the energy efficient wireless sensor networks. She is an IEEE Senior Member and a Registered Professional Engineer in the province of Ontario, Canada.

Alagan Anpalagan received the B.A.S., M.A.S., and Ph.D. degrees in electrical engineering from the University of Toronto, Canada in 1995, 1997, and 2001, respectively. Since August 2001, he has been with the Ryerson University, Toronto, Canada, where he cofounded *WINCORE* laboratory in 2002 and has been leading the WAN (wireless access and networking) R&D Group. Currently, he is an Associate Professor and Program Director for Graduate Studies. His research interests are, in general, wireless communication, mobile networks, and system performance analysis; and in particular, QoS-aware radio resource management, joint study of wireless physical/link-layer characteristics, cross-layer resource optimization, and wireless sensor networking. He has published more than 40 papers and articles in international conferences and journals in his research areas. He currently serves as IEEE Toronto Section Chair, previously served as Chair, Communications Chapter—IEEE Toronto Section (2004-2005) and Technical Program Cochair of IEEE Canadian Conference on Electrical and Computer Engineering (2004). His current editorial duties include Guest Editor on special issue on Radio Resource Management in 3G+ Wireless Systems (2005-2006) and Associate Editor in EURASIP Journal of Wireless Communications and Networking. He is an IEEE Senior Member and a Registered Professional Engineer in the province of Ontario, Canada.